Hsp70 Protects Against Peroxynitrite-Induced Inactivation of SERCA2a by Preventing Protein Oxidation and Aggregation

By

Christopher Vigna

A thesis
presented to the University of Waterloo
in fulfillment of the
thesis requirement for the degree of
Masters of Science
in
Kinesiology

Waterloo, Ontario, Canada, 2008

AUTHOR'S DECLARATION

I hereby declare that I am the sole author of this thesis. This is a true copy of the thesis, including any required final revisions, as accepted by my examiners.

I understand that my thesis may be made available electronically to the public.

Christopher Vigna

ABSTRACT

The purpose of this study was to examine the effects of exogenous peroxynitrite ($ONOO^-$) on the cardiac isoform of the sarco(endo)plasmic reticulum Ca^{2+}-ATPase (SERCA2a) and to determine if overexpression of heat shock protein 70 (Hsp70) could protect SERCA2a function. To characterize the interaction between SERCA2a and Hsp70, cDNAs encoding each protein were co-transfected in human embryonic kidney cells (HEK-293) using the calcium-phosphate technique. Western blotting confirmed the expression of SERCA2a and a ~1.9-fold overexpression of Hsp70 in HEK-293 cells. $ONOO^-$ was added chronically (250 μM bolus each minute for 10 minutes) to co-transfected HEK-293 cells in culture. Maximal Ca^{2+}-ATPase activity (V_{max}) was assessed on microsomal fractions isolated following exposure to $ONOO^-$. V_{max} was reduced by ~20% in HEK-293 cells transfected with SERCA2a alone (S2a-pMT2). When Hsp70 was co-transfected with SERCA2a (S2a-Hsp70), V_{max} was fully protected following incubation with $ONOO^-$. Western blot analysis showed that there were no changes in FITC binding capacity and 3-nitrotyrosine content in any of the groups. However, overexpression of Hsp70 prevented oxidation of SERCA2a, as assessed by reactive carbonyl content, following exposure to $ONOO^-$ when compared to S2a-pMT2. In addition, SERCA2a aggregation was lower compared to S2a-pMT2 groups under both control and $ONOO^-$ conditions. Co-immunoprecipitation of SERCA2a and Hsp70 confirmed that Hsp70 physically interacts with SERCA2a under all conditions. These results suggest that Hsp70 physically binds to SERCA2a and prevents oxidation and aggregation of SERCA2a, thus preserving enzyme activity.

ACKNOWLEDGEMENTS

I have called the University of Waterloo home for seven years, and have enjoyed each and every minute. From undergraduate to graduate studies, I have been surrounded by great friends who have made these the best years of my life.

I must acknowledge my supervisor, Dr. A. Russell Tupling, who has been a great influence and mentor of my academic career. Many hours were spent in his office discussing concepts, ideas and even current events. I look forward to my PhD. and future studies under the tutelage Dr. Tupling.

I must thank my fellow lab mates. Coming to work each day was a joy and not a chore because the atmosphere created by everyone was fun and enjoyable. I must specifically thank Eric Bombardier, Dr. M. H. Fu and Dr. T. Duhamel. These colleagues taught me essentially all the lab skills I have compiled to date and this thesis would not have been possible if it were not for them.

Not only are the 2nd floor research labs in BMH highly productive and well respected but they are also staffed with exceptional people. I must acknowledge my friends and colleagues in the Rush, Quadrilatero, Stark and Hughson labs.

Finally, and most importantly, I must thank my family. I was strongly encouraged to go to Waterloo so that I could "grow up" and mature. Through my experiences at Waterloo I found a career that is challenging, intriguing and constantly changing. Without my family's support I would have been able to make the strides necessary to accomplish what I have today.

DEDICATION

I dedicate this thesis to my family, whose love and support has helped me through my academic career.

TABLE OF CONTENTS

LIST OF FIGURES

LIST OF ABBREVIATIONS

$[Ca^{2+}]_f$	Cytosolic free Ca2+ concentration
$^{\cdot}OH$	Hydroxyl radical
3-D	Three dimension
3-NY	3-Nitrotyrosine
Å	Ångström
AAPH	2,2'-azobis(2-amidinopropane) dihydrochloride
A-Domain	Actuator domain
ADP	Adenosine diphosphate
APD	Ammonium peroxydisulfate
Asn	Asparagine
Asp	Aspartic acid
ATP	Adenosine triphosphate
BHT	Butylated hydroxytoluene
BSA	Bovine serum albumin
Ca^{2+}	Calcium
CaMKII	Ca2+/Calmodulin-dependent protein kinase
cAMP	Cyclic adenosine monophosphate
CLFS	Chronic low frequency stimulation
CPA	Cyclopiazonic acid
Cu/Zn-SOD	Copper/Zinc superoxide dismutase
Cys	Cysteine
DHPR	Dihydropyridine receptor
DNP	Dinitrophenyl
DNPH	2,4-dinitrophenylhydrazine
DTNB	5,5'-dithiobis(6-nitrobenzoic acid)
DTT	Dithiothreitol
EC	Excitation-contraction
EDL	Extensor digitorum longus
eNOS	Endothelial nitric oxide synthase
ER	Endoplasmic reticulum
FITC	Fluorescein isothiocyanate
Gln	Glutamine
Glu	Glutamic acid
GSH	Glutathione
H^+	Hydrogen ion/proton
H_2O	Water
H_2O_2	Hydrogen peroxide
HEK-293	Human embryonic kidney cells
HEPES	4-(2-hydroxyethyl)-1-piperazineethanesulfonic acid
HPLC-MS	High performance liquid chromatography-mass spectroscopy
Hsp	Heat shock protein

Ile	Isoleucine
IP	Immunoprecipitation
IR	Ischemia-reperfusion
kDa	Kilo daltons
L6	Rat myogenic cell line
LDH	Lactate dehydrogenase
Lys	Lysine
Met	Methionine
Mg^{2+}	Magnesium
MHC	Myosin heavy chain
MLC	Myosin light chain
Mn-SOD	Manganese superoxide dismutase
mRNA	Messenger ribonucleic acid
NADH	Nicotinamide adenine dinucleotide
NBD	Nucleotide binding domain
N-Domain	Nucleotide domain
NEF	Nucleotide exchange factor
NFAT	Nuclear factor of activated t cells
NF-SLN	N-terminally FLAG tagged sarcolipin
nNOS	Neuronal nitric oxide synthase
$NO\cdot$	Nitric oxide
$O2^{\cdot-}$	Superoxide anion
$ONOO^-$	peroxynitrite
pAsp	Phosphorylated Aspartic acid
PBS	Phosphate buffered saline
P-Domain	Phosphorylation domain
PEP	Phophoenol pyruvate
Phe	Phenylalanine
P_i	Phosphate
PK	Pyruvate kinase
PKA	Protein kinase A
PLN	Phospholamban
PMSF	Phenylmethylsulphonyl fluoride
PVDF	Polyvinyldiene difluoride
RNS	Reactive nitrogen species
ROS	Reactive oxygen species
RSSR	Disulfide
RyR	Ryanodine receptor
S2a-Hsp70	HEK-293 co-transfected with SERCA2a and Hsp70 cDNA
S2a-pMT2	HEK-293 co-transfected with SERCA2a and pMT2 cDNA
SBD	Substrate binding domain
SDS-PAGE	Sodium dodecyl sulphate polyacrylamide gel electrophoresis
SE	Standard error of the mean

Ser	Serine
SERCA	Sarco(endo)plasmic reticulum Ca2+-ATPase
SH	Sulfhydryl
SLN	Sarcolipin
SR	Sarcoplasmic reticulum
T_3	3,5,3'-triiodo-L-thyronine
TA	Tibialis anterior
TBS-T	Tris buffered saline plus Tween-20
Thr	Threonine
TR	T3 receptors
Trp	Tryptophan
TT	Transverse-tubule
Tyr	Tyrosine
V_{max}	Maximal Ca2+-ATPase activity

Introduction

The role of sarcoplasmic reticulum in excitation-contraction coupling.

Human locomotion results from a coordinated sequence of contraction and relaxation of skeletal muscles. The molecular series of events that give rise to a contraction and relaxation cycle have been characterized and are termed excitation-contraction (EC) coupling. In brief, EC coupling begins with motor nerve innervation, which depolarizes the sarcolemma. Depolarization propagates within the muscle via the transverse-tubule (TT) network, thus activating the voltage sensitive dihydropyridine receptor (DHPR). DHPR activation causes opening of the ryanodine receptor (RyR), which allows calcium (Ca^{2+}) to move down its concentration gradient from the sarcoplasmic reticulum (SR) to the cytosol. A rise in cytosolic free Ca^{2+} concentration ($[Ca^{2+}]_f$) relieves tropomyosin inhibition and allows activation of the contractile apparatus (actin-myosin). In order for relaxation to occur the sarco(endo)plasmic reticulum Ca^{2+}-ATPase (SERCA) must pump large amounts of Ca^{2+} back into the SR. The regulation of Ca^{2+} release and sequestration from the SR is vital for proper EC coupling.

The SR is a membranous network, which surrounds the actin and myosin filaments within skeletal muscle cells. A key structural characteristic of the SR is the formation of a triad. Triads are composed of a TT invagination flanked by two SR terminal cisternae, which represents the functional calcium release unit. In this region there is a high density of DHPRs (located within the TT membrane), RyRs (located within the SR membrane) and calsequestrin molecules, which are intimately associated with RyRs in the lumen of the SR. The DHPR and RyR form highly organized series of arrays consisting of 4 DHPRs physically interacting with every other RyR (for review see; Protasi, 2002). Although

SERCAs are present at the terminal cisternae, they are most abundant along the longitudinal SR, an area that flanks the contractile apparatus.

3-dimensional structure of SERCA and its reaction cycle.

The SERCA is a ~100 kDa integral membrane protein whose primary function is to pump 2 mol Ca^{2+} from the cytosol to the lumen of the SR at the expense of 1 mol ATP. The amino acid sequence of SERCA was first deduced by MacLennan and colleagues (1985). These researchers predicted several domains that comprise SERCA, those being the transmembrane domain (10 helices; M1-10), the actuator domain (A-domain), the nucleotide binding domain (N-domain) and the phosphorylation domain (P-domain) (MacLennan et al., 1985). A decade and a half later, Toyoshima and co-workers (2000) confirmed the predictions of MacLennan and colleagues (1985) when they successfully crystallized and resolved, with high resolution, the 3-dimensional (3-D) structure of SERCA1a using rabbit fast-twitch skeletal muscle (Toyoshima et al., 2000).

Chikashi Toyoshima's group has revolutionized the understanding of the structure-function relationships between the domains of SERCA and how each contributes to the pumping of Ca^{2+} across the SR membrane. A simplified schematic of the reaction cycle of SERCA is displayed in Figure 1. In brief, when the Ca^{2+} binding pocket is open to the cytosol the enzyme is in the E1 state and Ca^{2+} will bind to SERCA in a cooperative fashion. Ca^{2+} binding permits ATP to bind to the N-domain. Subsequently, SERCA is autophosphorylated and undergoes conformational changes, which exposes the Ca^{2+} binding pocket to the lumen of the SR (E2 conformation). Next, the two Ca^{2+} ions are expelled, the phosphate (P_i) is hydrolyzed and SERCA transitions from the E2 → E1 state.

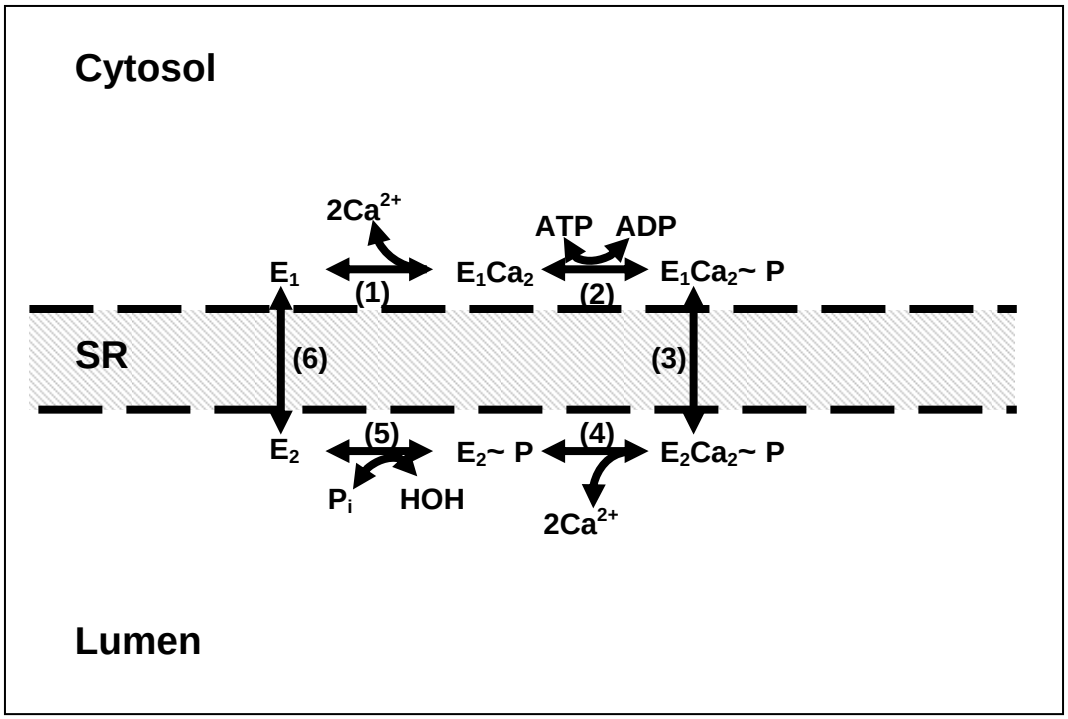

Figure 1: A simplified schematic of the reaction cycle of SERCA. This image was adapted from Mall et al. *J. Biol. Chem.* 281(48): 36597-36602, 2006.

At the present time there are approximately 20 crystal structures of SERCA in 7 different states, which has resolved the entire reaction cycle of SERCA in 3-D (for review see; Toyoshima, 2007; Toyoshima, 2008). The four main crystal structures that comprise the reaction cycle of SERCA can be seen in Figure 2. When SERCA is in the E2 state, Ca^{2+} displaces H^+ and H_2O in the Ca^{2+} binding pocket. The first Ca^{2+} forms bonds with side chain oxygen atoms from Asn768, Glu771 (M5), Thr799, Asp800 (M6), Glu908 (M8) and two water molecules (Toyoshima, 2008). The second binding site utilizes oxygen atoms from Asn796, Asp800 (M6) and two from Glu309, which acts as the gating residue. The sequential binding of two Ca^{2+} ions causes the M5 alpha helix, the mast of SERCA, which links the transmembrane domain to the P-domain, to straighten. This conformational change in M5 initiates separation of the 3 cytoplasmic domains, which were in close proximity in the E2 state and permits ATP to bind to the N-domain (Toyoshima, 2007).

The next step involves the N-domain "capping" or covering the P-domain, which is accomplished through the formation of numerous hydrogen bonds around the ATP and Mg^{2+}, which links the N-domain and the P-domain. This puts strain on the cytosolic headpiece and causes a deflection of the A-domain. These structural changes cause the M1 helix to be partially pulled out of the SR membrane and puts a slight bend in the M1 helix. This action closes the cytoplasmic Ca^{2+} gate (Glu309) and thus occludes the two Ca^{2+} within the transmembrane domain (Toyoshima, 2007).

The γ-phosphate of ATP is transferred to Asp351 and ADP dissociates from SERCA, which initiates the separation of the P- and N-domains (Toyoshima, 2007). In order to prevent ADP from binding to the N-domain and to restrict access of water to the aspartylphosphate, the A-domain rotates 110^o and wedges its TGES loop into the space

formerly occupied by ADP. These large movements by the A-domain are transmitted to helices M1-6, which opens the lumenal gate allowing the bound Ca^{2+} to be released into the SR lumen. Once released 2-3 H^+ and water molecules enter the Ca^{2+} binding pocket in order to stabilize the region. The H^+ are deposited in the cytosol, but a proton gradient is not generated due the permeability of the SR membrane to protons.

Hydrolysis of the aspartylphosphate is mediated by further rotation of the A-domain, which through conformational changes of the TGES loop and Glu183 allows a water molecule access to Asp351. Glu183 plays a critical role in hydrolysis as it abstracts a H^+ from water, thus permitting hydrolysis of pAsp351 (Anthonisen et al., 2006; Toyoshima, 2008). When the P_i and Mg^{2+} are released the strain placed on the P-domain is relieved, which is transmitted to M1, M2 and M4 and causes the closure of the luminal Ca^{2+} gate (Toyoshima, 2007). The reaction cycle can now proceed again with the binding of Ca^{2+} to its binding pocket.

The resolution of SERCA1a crystal structures has highlighted the large scale movements that are required to transmit the energy derived from Asp351 phosphorylation in the P-domain nearly 50 Å to the Ca^{2+} binding pocket in the transmembrane domain. All of these crystallography studies have examined SERCA1a the fast-twitch isoform in adult skeletal muscles. However, there exist several other critical SERCAs that are homologous to SERCA1a.

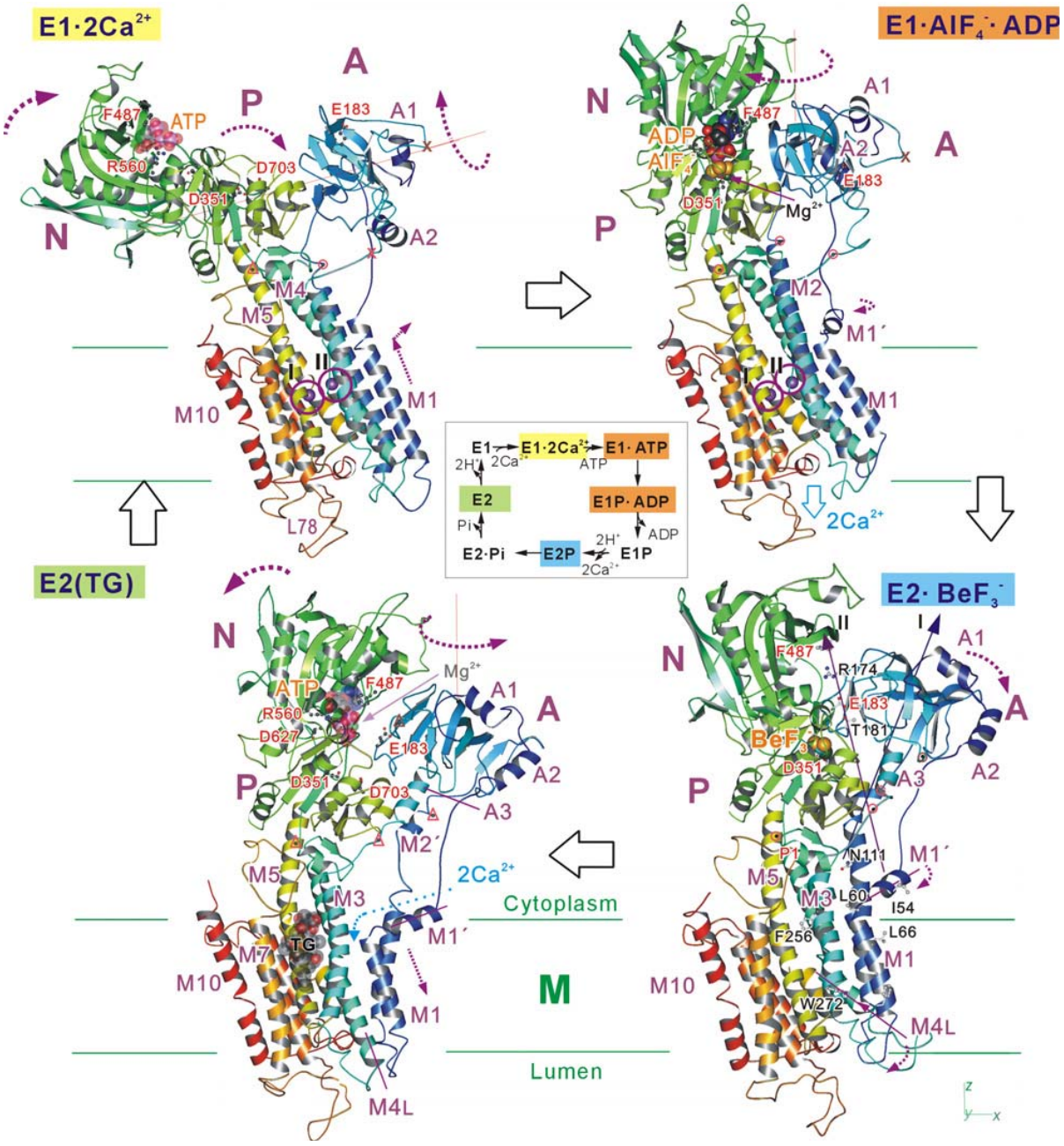

Figure 2: Detailed 3-dimensional representation of the reaction cycle of SERCA. From Toyoshima C. *Arch. Biochem. Biophys.* 476(1): 3-11, 2008. The inset identifies the corresponding intermediates within the reaction cycle that the 3-D SERCA1a structures represent. Refer to text for description of the reaction cycle.

SERCA genes and isoforms.

At the genomic level, there are three *ATP2A* genes that encode multiple SERCA isoforms (Pan et al., 2003; MacLennan et al., 1985; Lytton & MacLennan, 1988; Brandl et al., 1986; Burk et al., 1989). Each gene gives rise to two or more alternatively spliced gene transcripts, which are ultimately translated into their respective proteins. For example the *ATP2A1* gene codes for SERCA1b, the isoform abundant in neonatal skeletal muscle and SERCA1a, which is the predominant isoform in adult fast-twitch skeletal muscle (Pan et al., 2003; Wu & Lytton, 1993). SERCA2a is the exclusive isoform expressed in cardiac muscle and is present in adult slow-twitch muscle, whereas SERCA2b is the primary isoform in vascular smooth muscle. SERCA3 variants are expressed more ubiquitously. Recently, a third SERCA2 isoform, SERCA2c has been characterized (Dally et al., 2006). The expression pattern of SERCA2c appears to mimic that of SERCA2a, yet the maximal catalytic activity of SERCA2c is nearly identical to that of SERCA2b (Dally et al., 2006). Using immunocytochemistry of fixed human cardiac tissue these authors found that SERCA2c was compartmentalized to regions in the SR that are close to the sarcolemma. The study by Dally and co-workers (2006) found that SERCA2c is expressed in distinct areas of the myocyte and at far lower levels when compared to SERCA2a.

Manipulation of SERCA isoform expression by chronic low frequency stimulation.

Since the identification of the genes encoding SERCAs, the regulation of these genes and the associated protein expression has been highly investigated. Two models commonly employed to alter SERCA1a and SERCA2a expression in skeletal muscle are altered thyroid status (i.e. induced hypo/hyperthyroidism) and chronic low frequency stimulation (CLFS).

When applied to a fast-twitch skeletal muscle, CLFS leads to a progressive shift in fibre type to that of a slow-twitch phenotype (Pette & Düsterhöft, 1992). One of the major transformations associated with CLFS is a shift in both myosin heavy (MHC) and light chain (MLC) isoforms from Type II to Type I (Leeuw & Pette, 1996). During CLFS there is a parallel shift in SERCA isoform when compared to that of the MHC isoform, namely the fast isoform, SERCA1a is down regulated and the slow isoform, SERCA2a is up regulated (Pette & Düsterhöft, 1992). Studies indicate that prior to a significant alteration in the SERCA pool, there is a robust reduction in the maximal Ca^{2+}-ATPase activity (V_{max}) in the first hours and days of CLFS in the extensor digitorum longus (EDL) and tibialis anterior (TA) muscles of rat and rabbit (Klebl et al., 1998; Matsunaga et al., 2001). These studies point to protein oxidation as the likely mechanism associated with the reduction in ATPase activity. In addition, the reduction in enzyme activity measured *in vitro* is likely underestimated considering the pronounced reduction in phosphorylation potential observed during CLFS *in vivo* (Green et al., 1992).

It was initially believed that the signal responsible for activating the shift in gene expression of chronic low-frequency stimulated muscles was the pronounced and sustained drop in phosphorylation potential (Pette & Dusterhoft, 1992). Elevations in $[Ca^{2+}]_f$ were thought to be secondary since the rise in $[Ca^{2+}]_f$ was delayed and transient. However,

improvements in the sensitivity of Ca^{2+} fluorophores permitted the measurement of $[Ca^{2+}]_f$ in muscles during CLFS in the basal state and during contractions (Carroll et al., 1999). Carroll and colleagues (1999) found that the resting $[Ca^{2+}]_f$ in single fibres from rat EDL exposed to CLFS rose significantly within the first 12 hrs of stimulation and remained elevated during the 10-day protocol. It is now believed that Ca^{2+} plays a significant role in initiating gene transcription and/or silencing (Chin et al., 1998).

Ca^{2+} signaling and gene regulation.

Persistent elevations in $[Ca^{2+}]_f$ activate calcineurin, a Ca^{2+}/Calmodulin-dependent serine/threonine phosphatase (Chin et al., 1998). Calcineurin has been termed the master regulator of fast-to-slow twitch fibre type shifts (Röckl et al., 2008). Activation of calcineurin, initiated by the binding of Ca^{2+} to the calmodulin-calcineurin complex, increases its phosphatase activity. The primary substrate of calcineurin is the nuclear factor of activated t cells (NFAT) transcription factors (Chin et al., 1998). Once dephosphorylated, NFAT translocates to the nucleus where it activates the "slow-fibre program" of genes (Chin et al., 1998). Thus, Ca^{2+} itself is a potent stimulus for induction of fibre type shifts and changes in SERCA expression. However, other signals partially independent of significant perturbations to $[Ca^{2+}]_f$ can induce changes in SERCA expression patterns.

Regulation of SERCA expression by thyroid hormone.

Artificial induction of hypo- and hyperthyroidism has a profound influence on SERCA isoform expression, particularly SERCA1a. Early studies in a myogenic cell line developed from rat (L6) demonstrated that administration of 5 nM 3,5,3'-triiodo-$_L$-thyronine (T_3) resulted in an increase in SERCA1a protein by ~160% (Thelen et al., 1994). This study also found that SERCA1 mRNA was elevated by ~240%, suggesting that T_3 can regulate SERCA1a at the genomic level. Studies examining the effects of thyroid status on rabbit soleus muscles indicate that hypothyroidism results in large reductions (50-80%) in SERCA1a protein and only a modest attenuation (~30%) of SERCA2a (Van Der Linden et al., 1996; Arruda et al., 2005). Conversely, hyperthyroidism can induce massive elevations in SERCA1a content (2-6 fold), and cause significant reductions in SERCA2a content ranging from 30-70% (Van Der Linden et al., 1996; Yamada et al., 2004; Arruda et al., 2005).

The mechanisms associated with SERCA gene expression and thryoid status are complex and well documented (for review see; Simonides et al., 2001). T_3 stimulated transcription of *SERCA1* requires T_3 binding to a T_3-receptor (TR) (Simonides et al., 2001). The primary TRs in skeletal muscle are TRα1 and TRβ1. Once activated these receptors bind to the thyroid hormone response element on the *SERCA1* gene and potentiate transcription. Interestingly, $[Ca^{2+}]_f$ may influence the efficacy of T_3-induced SERCA1a expression. Muller and colleauges (1992) showed that the stimulatory effect of T_3 on SERCA1a expression at a $[Ca^{2+}]_f$ of 120 nM was nearly abolished at 185 nM. Considering the rise in $[Ca^{2+}]_f$ during CLFS, a suppression of the stimulatory effect of endogenous T_3 may contribute, in part, to the down regulation of SERCA1a.

Post-translational regulation of SERCA.

Post-translational regulation of SERCA is mediated by two small proteolipids, sarcolipin (SLN) and phospholamban (PLN), that are respectively, 31 and 52 amino acids in length (Wawrzynow et al., 1992; Fujii et al., 1987). The existence of SLN was first observed by MacLennan and co-workers (1972), who noted a protein with an apparent molecular mass of ~6 kDa that co-purified with the Ca^{2+}-ATPase of rabbit skeletal muscle (Odermatt et al., 1998). SLN and PLN possess similarity in their genes, which results in significant conservation of amino acid residues between the two proteins. Therefore, it has been proposed that the SLN and PLN genes are members of a family (Odermatt et al., 1997).

Manipulation of thyroid status and chronic contractile activity can alter the gene expression of SLN and PLN. Studies have found that CLFS for only 3-7 days initiates transcription of both SERCA2a and PLN genes with an apparent decrease in transcription of the SERCA1a gene (Hu et al., 1998). However, a study by Odermatt and colleagues (1998) found that 3-4 days of CLFS caused no change in SERCA1a protein, but there was an ~40% decrease in SLN protein. In the heart, hypothyroidism attenuates SERCA2a content whereas hyperthyroidism increases SERCA2a protein (Kiss et al., 1994; Shenoy et al., 2001). The opposite is true for PLN. Hypo- and hyperthyroidism results in the increase and attenuation of PLN, respectively (Kiss et al., 1994; Holt et al., 1999; Shenoy et al., 2001).

Until recently, attempts to develop an antibody for SLN have been unsuccessful (Vangheluwe et al., 2005). This has resulted in the majority of knowledge about SLN expression being derived from mRNA levels in tissue. However, what appears to be a viable SLN antibody (i.e. does not cross react with PLN) has been developed (Babu et al., 2007). As previously thought, SLN is highly expressed in atria and undetectable in ventricle, where

PLN expression is robust (Babu et al., 2007). The notion that SLN and PLN respectively, are expressed in fast- and slow-twitch skeletal muscle has been an oversimplification as SLN and PLN are co-expressed in the soleus of mouse, rat and rabbit (Babu et al., 2007). Characterizing the expression pattern of SLN and PLN in skeletal muscle is important from a structure-function perspective as their influence on SERCA is largely dependent on the ratio of SERCA to SLN and/or PLN (Mall et al., 2006).

The structures of SLN and PLN are similar in their transmembrane regions. Each protein has a single transmembrane α-helix. This highly conserved region corresponds to amino acids 22-52 and 8-26 in PLN (domain II) and SLN, respectively (Sugita et al., 2006; Bhupathy et al., 2007). Disparity in the structure of SLN and PLN arises in the N- and C-terminus regions. PLN exhibits a second α-helix (domain Ia) in the N-terminal sequence (amino acids 1-16) that physically interacts with SERCA2a (Tada & Toyofuku, 1996; Sugita et al., 2006). The cytoplasmic domain Ia of PLN is linked to the transmembrane domain II by a less structured, more flexible link (domain Ib) composed of 5 amino acids (Sugita et al., 2006). Interaction between SLN and SERCA1a has been shown to occur with the highly conserved RSYQY lumenal domain of SLN and Phe73, Trp77, Ile85 and Phe88 of SERCA1a (Hughes et al., 2007). Furthermore, SLN's RSYQY domain (C-terminus) appears vital for compartmentalization of SLN within the ER/SR membrane, as demonstrated in HEK-293 cells co-transfected with NF-SLN (N-terminally FLAG tagged SLN) and SERCA cDNAs (Gramolini et al., 2004).

Through their interactions with SERCA, PLN and SLN decrease the apparent affinity of SERCA for Ca^{2+}. Inhibition is alleviated when $[Ca^{2+}]_f$ is elevated or through phosphorylation of PLN or SLN. Phosphorylation of PLN at Ser16 by cAMP-dependent

protein kinase A (PKA) and/or at Thr17 by Ca^{2+}/Calmodulin-dependent protein kinase (CaMKII) reverses the inhibitory protein-protein interaction between PLN and SERCA2a (MacLennan et al., 2002; Morita et al., 2008). Recently, it was demonstrated that SLN may be phosphorylated in the hearts of mix bred NF-SLN transgenic and PLN knock-out mice (Gramolini et al., 2006). These authors found that SLN phosphorylation may occur at Ser4 or Thr5 via a Serine/Threonine Kinase 16. However, the ability of SLN to be phosphorylated within skeletal muscle has yet to be determined.

Extensive work investigating the structure and function relationship between SLN, PLN and SERCA has been performed by David MacLennan's group. They have utilized HEK-293 cells as a host to express these proteins and have performed a plethora of mutagenesis and cross-linking experiments to model specific interaction sites among these proteins (Traaseth et al., 2008). Structurally, PLN exists as inactive pentamers or as active monomers interacting with available SERCA molecules. Typical interactions between SERCA and PLN or SLN occur as heterodimers. However, when SLN, PLN and SERCA1a or SERCA2a are expressed together in HEK-293 cells, super inhibition of Ca^{2+}-ATPase activity occurs (Odermatt et al., 1998; Asahi et al., 2002). Asahi and colleagues (2002) demonstrated that the presence of SLN increased the monomer:pentamer ratio (i.e. increased the number of active PLN molecules). Furthermore, SLN was found to physically interact with PLN and stabilize PLN binding to SERCA, which likely contributed to the super inhibition (Asahi et al., 2002). When SERCA1a is in the E2 conformation, PLN, SLN or both PLN-SLN can bind to SERCA1a in a groove formed by the transmembrane helices M2, M4, M6 and M9 (Morita et al., 2008; Asahi et al., 2003). Cross-linking studies demonstrate that PLN can interact with SERCA1a at multiple sites (Lys3 on PLN and Lys397, 400 on

SERCA1a; Gln23 on PLN and Lys328 on SERCA1a) (Toyoshima et al., 2003; Morita et al., 2008). Once phosphorylated it is believed that salt bridges form between the P_i and amino acids Arg9, 13 and/or 14 of PLN, which alters the conformation within domain Ia of PLN and causes it to dissociate from SERCA (Sugita et al., 2006).

At saturating Ca^{2+} concentrations, PLN does not influence the V_{max} of SERCA2a. However, the effect SLN on the V_{max} of SERCA1a remains somewhat contentious. An early study by Odermatt and colleagues (1998) found that NF-SLN co-transfected with SERCA1a into HEK-293 cells resulted in stimulation of V_{max}. However, further investigation by the same group suggested that SLN did not significantly alter V_{max} of SERCA1a (Asahi et al., 2002). Furthermore, when SLN was reconstituted with SERCA1a in lipid, a decrease in V_{max} of ~20% occurred (Hughes et al., 2007). It is evident that there are methodological implications for measuring V_{max} of SERCA in the presence of SLN. It appears that the lipid environment and the ratio of SERCA:SLN are critical. Conceivably, SLN does not influence V_{max} of SERCA1a, given the homology between PLN and SLN and the fact that PLN has no effect on SERCA V_{max}.

Oxidative stress and SERCA function.

Oxidative stress caused by ageing, hyperthermia, ischemia-reperfusion (IR), certain disease states and exercise can modify SERCA post-translationally. Several studies have utilized heat stress and exercise as models of oxidative stress, in order to examine the effects on SERCA function. Indeed, exercise of various modalities has deleterious effects on SR Ca^{2+} handling in humans (Hill et al., 2001; Tupling et al., 2000; Leppik et al., 2004) and in rodents (Inashima et al., 2003; Holloway et al., 2006) when assessed *in vitro*. However, one

study that utilized isometric contractions (Sahlin et al., 2006) and another that used eccentric contractions (Nielsen et al., 2005), failed to observe significant reductions in SR Ca^{2+}-uptake. Moreover, repeated electrical stimulation of rat hind-limb and exercise have been shown to increase SERCA activity in muscles of low oxidative potential (Ferrington et al., 1996; Holloway et al., 2006). Explanations as to the mechanisms responsible for reduced Ca^{2+}-ATPase activity following exercise have ranged from alterations in ATP concentration (de Meis & Sorenson, 1989), glycogen (Lees et al., 2003) and changes in pH (Mandel et al., 1982; Matsunaga et al., 2003). However, there is a growing body of evidence suggesting that reactive oxygen species (ROS) generated during exercise may contribute to the reductions in Ca^{2+}-ATPase activity.

Exercise potentiates the generation of ROS and reactive nitrogen species (RNS) in skeletal muscle. Kobzik and co-workers (1994) were the first to demonstrate that neuronal nitric oxide synthase (nNOS) is present in mammalian skeletal muscle. That study also demonstrated that nitric oxide ($NO^{\cdot}$) production and/or $NO^{\cdot}$ intermediates accounted for ~33% of the reducing equivalents generated in resting diaphragm whereas superoxide anion ($O_2^{\cdot-}$) did not contribute significantly to the reduction of cytochrome c (Kobzik et al., 1994). However, during muscle contraction, $O_2^{\cdot-}$ was the predominant reducing equivalent contributing to the reduction of cytochrome c. $O_2^{\cdot-}$ can be dismutated enzymatically into hydrogen peroxide (H_2O_2) in the mitochondria and cytosol by manganese superoxide dismutase (Mn-SOD) and Cu/Zn-SOD, respectively. If Mn- and Cu/Zn-SOD fail to clear the cell of $O_2^{\cdot-}$ then it may react with other ROS/RNS, proteins or lipids. For example, the reaction of $NO^{\cdot}$ and $O_2^{\cdot-}$ is extremely rapid, with a rate constant of $1.9 \pm 0.2 \times 10^{10}$ $M^{-1} \cdot s^{-1}$ (Kissner et al., 1997) and produces the highly reactive peroxynitrite ($ONOO^-$).

SERCA1a and SERCA2a contain 24 and 26 cysteine (Cys) residues, respectively, making SERCAs highly susceptible to oxidative stress (Tupling et al., 2007). Numerous studies have characterized the effects of ROS on SERCA activity *in vitro*. An early study by Scherer and Deamer (1986) incubated SR fractions isolated from lobster and rabbit skeletal muscle with ammonium peroxydisulfate (APD) and found that SERCA activity was reduced by approximately 39%. This study also found that the sulfhydryl (SH) content of SR fractions incubated with APD was reduced significantly, as determined by the DTNB assay. Reductions in SERCA activity were not alleviated by incubation with anti-oxidants but incubation with strong reducing agents (dithiothreitol; DTT or mercaptoethanol) protected enzyme function (Scherer & Deamer, 1986). Consistent with the results from the study by Scherer and Deamer (1986), other studies have found that incubation of enriched SR with hypochlorus acid (Favero et al., 1998), $FeSO_4$/EDTA (Kaplan et al., 2003) or diamide (Senisterra et al., 1997) reduced Ca^{2+}-ATPase activity significantly, which was associated with reductions in free SH content. However, several studies have shown that ROS-induced inactivation of SERCAs can occur in the absence of SH oxidation (Castilho et al., 1996; Viner et al., 1997). Alternative mechanisms of inactivation include protein fragmentation and/or protein aggregation (Castilho et al., 1996;Viner et al., 1997).

Protein aggregation could lead to the development of high molecular weight aggregates, which can be visualized by sodium dodecyl sulphate polyacrylamide gel electrophoresis (SDS-PAGE) and Western blotting (Castilho et al., 1996). Evidence that SERCAs form aggregates suggests that multiple SERCAs form intermolecular bonds or that a single SERCA pump can cross-link with other SERCAs or smaller SERCA fragments. It has been suggested that disulfide (RSSR) bonds formed between SERCA molecules are

responsible for the development of high molecular weight aggregates (Senisterra et al., 1997). However, Viner and colleagues (1997) proposed that formation of RSSR bonds was not responsible for SERCA aggregation and suggested the likely mechanism was bityrosine formation. It appears that the assay conditions and the type of oxidant used may influence the mechanism by which inactivation of SERCA occurs.

A mechanism associated with reduced Ca^{2+}-ATPase activity following ROS exposure that has gained support in recent years is damage to the N-domain of SERCA. The headpiece of SERCA requires a great deal of mobility in order to proceed through a reaction cycle, particularly in the N-domain. Therefore, if the N-domain is compromised structurally, the ability of ATP to bind to SERCA and phosphorylate Asp351 may be reduced, which would result in depressed ATPase activity. An elegant study by Xu and colleagues (1997) found that if SR vesicles were pre-incubated with 1 mM ATP for 3 min prior to exposure to hydroxyl radical ($^{\bullet}OH$) that Ca^{2+}-ATPase activity was fully protected. The authors suggested that ATP bound to SERCA protected crucial amino acids near Asp351 from oxidation, and that Cys349 is a likely candidate for protection (Xu et al., 1997). Indeed, the N-domain of SERCA1a contains 7 Cys residues (MacLennan et al., 1985) and is therefore a potential target of ROS induced oxidation. Furthermore, incubation of isolated SR with hypochlorus acid reduced fluorescein isothiocyanate (FITC) binding to SERCA in a concentration dependent manner (Favero et al., 1998). FITC is used as a marker of the structural integrity of the N-domain of SERCA, since FITC covalently binds to Lys515 on SERCA1a, which is in close proximity to the nucleotide binding site (Abu-Abed et al., 2002). However, FITC is a crude marker of structural alterations to SERCA and provides no detail of the specific amino acids that are modified by oxidative stress.

Site specific modification to SERCA by ROS/RNS.

The development of proteomic techniques by Christian Schöneich's group has vastly improved the understanding of how ROS/RNS inhibit SERCA by identifying specific residues that are modified within the amino acid sequence of SERCA. In a study by Viner and colleagues (1999a), SERCA1a was exposed to varying concentrations of $ONOO^-$, the amount of oxidized Cys residues was determined and the amino acid sequence of tryptic fragments were analyzed using an HPLC-MS system. They found a progressive decrease in the amount of reduced Cys residues with increasing concentrations of $ONOO^-$. HPLC-MS analysis revealed that 100 μM $ONOO^-$ oxidized Cys614, 498, 525, 471, 344, 349 and based on their functional measures of SERCA1a ATPase activity and other experiments they confirmed the hypothesis of Xu and co-workers (1997), that reduced Cys349 is critical for proper enzyme function.

In a similar study, SR fractions isolated from rabbit fast-twitch skeletal muscle were exposed to DEA/NO (a $NO^\cdot$ donor) *in vitro* and the oxidation of Cys residues on SERCA1a was assessed (Viner et al., 2000). Incubation of SERCA1a with 0.1 mM DEA/NO lead to a greater number of Cys residues being oxidized when compared to their previous study, which utilized $ONOO^-$ (Viner et al., 1999a). In total, $NO^\cdot$ oxidized 13 Cys residues on SERCA1a whereas $ONOO^-$ only oxidized 6 Cys residues. These authors suggested that the majority of Cys residues oxidized are not critical for enzyme activity and that they may represent "endogenous" antioxidants for the enzyme (Viner et al., 2000). This concept was echoed by Grover et al., (1997), who attributed the greater susceptibility of SERCA2b than SERCA3 to H_2O_2 induced inactivation as a result of differences in their Cys content. SERCA2b and SERCA3 contain 29 and 25 Cys residues, respectively (Grover et al., 1997). However, it was

not known how many Cys residues were oxidized on each SERCA isoform or whether critical Cys residues in SERCA2b and SERCA3 were compromised (Grover et al., 1997). Although SERCA isoforms have a high degree of sequence homology, these studies suggest that slight variations in amino acid sequence (i.e. number of Cys residues) and/or 3-D conformation may confer different levels of susceptibility to oxidative stress.

The cardiac isoform of SERCA, namely SERCA2a, shares 84% homology with SERCA1a (Viner et al., 1999b), yet SERCA2a more readily undergoes nitration of tyrosine (Tyr) residues when compared to SERCA1a (Sharov et al., 2002). SERCA1a shares 16 out of the 18 Tyr residues of SERCA2a, yet only Tyr122 is nitrated on SERCA1a following exposure to $ONOO^-$ (Sharov et al., 2002). The effects of ageing on amino acid residues of SERCA1a have shown that Cys is preferentially oxidized, encompassing at least 10 Cys residues (Sharov et al., 2006). In young rat heart, SERCA2a contained 3-nitrotyrosine (3-NY) residues at Tyr122, 130, 497, 586, 990 and as animals aged Tyr294, 295, 753 were further nitrated (Knyushko et al., 2005). Nitration of Tyr294 and Tyr295 appears to heavily influence the catalytic activity of SERCA2a as these amino acid residues are in close proximity to the Ca^{2+} binding sites (Knyushko et al., 2005). Taken together, these studies suggest there are critical amino acids that are altered by ageing (*in vivo* oxidative stress) or exogenous ROS/RNS (*in vitro*), which depends on the oxidant and the SERCA isoform in question.

Regardless of the oxidant used, a common methodological approach to investigating the effects of ROS on SERCA function has been to incubate samples with a single bolus of ROS for a given period of time and then perform functional measurements. A novel study by Gutiérrez-Martin and co-workers (2004) compared the effects of a single bolus of $ONOO^-$

compared to many smaller sequential additions of $ONOO^-$ on SR isolated from rabbit fast-twitch skeletal muscle. In physiological conditions the half-life of $ONOO^-$ is <0.1 sec. Therefore, in the "chronic" condition the concentration of $ONOO^-$ would likely be maintained at a higher concentration when compared to the acute bolus condition. In both conditions the final concentration of $ONOO^-$ was identical, however, the reduction in SERCA1a activity was exacerbated in the chronic exposure condition (Gutiérrez-Martin et al., 2004). These authors attributed the reductions in Ca^{2+}-ATPase activity to Tyr nitration and Cys oxidation, which is supported by their observation that epicatechin (blocker of tyrosine nitration) and glutathione (GSH) fully protected enzyme activity. However, no comparison between the degree of Cys oxidation and Tyr nitration were made between the acute and chronic $ONOO^-$ conditions. Therefore, further investigation into the mechanisms responsible for the potentiated reduction of Ca^{2+}-ATPase activity in the chronic $ONOO^-$ condition is warranted.

Protection of SERCA function from oxidative stress.

Prevention or attenuation of ROS induced damage of SERCAs could have functional benefits *in vivo* (i.e. improve contractile function following an acute stress). The potential protective effects of anti-oxidants on SR Ca^{2+}-ATPase activity exposed to ROS have been investigated *in vitro* (Moreau et al., 1998; Kaplan et al., 2003). The deleterious effects of $FeSO_4$/EDTA on SERCA2a ATPase activity were almost completely reversed when pre-incubated with either butylated hydroxytoluene (BHT; lipid soluble anti-oxidant) or glutathione (GSH; water soluble) (Kaplan et al., 2003). Another study observed that only partial protection of SERCA1a was afforded by DTT and GSH after incubation with HOCl

(Favero et al., 1998). On the contrary, pre-incubation with BHT or DTT failed to protect SERCA activity following exposure to $^{\bullet}OH$ (Moreau et al., 1998). It would appear that if the oxidative stress were too severe, then antioxidants and reducing agents could not prevent or reverse oxidative damage to SERCA and maintain proper enzyme function.

Structure and function of heat shock protein 70.

Eukaryotic cells possess an innate mechanism for protection against oxidative stress induced protein damage. Heat shock proteins (Hsps) are members of a highly conserved family of proteins that possess a variety of functions, but are best known for chaperoning and folding nascent peptides and re-folding partially denatured proteins (Welch, 1992; Liu et al., 2006). Hsp70 and Hsp60 are localized respectively, in the cytosol and mitochondria, and are vital for proper folding and re-folding of proteins. The highly inducible form, Hsp70 is rapidly upregulated in cardiac and skeletal muscle following bouts of exercise (Milne & Noble, 2002), hyperthermia (Ruell et al., 2004) and mild IR (Trost et al., 1998). Elevation of Hsp70 in response to a mild stress can provide cyto-protection from subsequent potentially lethal stress, a phenomenon termed preconditioning (Yamashita et al., 1997).

Human Hsp70 is a 640 amino acid cytosolic protein, which possesses two distinct domains (Sriram et al., 1997). The N-terminal domain is 388 amino acids in length (44 kDa) and is referred to as the nucleotide binding domain (NBD) (Sriram et al., 1997; Goloubinoff & De Los Rios, 2007). The C-terminal region is the 28 kDa substrate binding domain (SBD) (Goloubinoff & De Los Rios, 2007). This region can be further subdivided into the actual 18 kDa SBD and the 10 kDa regulatory domain, which regulates ATP hydrolysis (Sriram et al., 1997).

For efficient ATPase turnover and substrate folding, Hsp70 relies on several co-chaperones. Hsp40 stimulates ATP hydrolysis by Hsp70 and aids in the targeting of substrates. The nucleotide exchange factors (NEFs) facilitate the release of ADP and the subsequent binding of an ATP molecule (Liu & Hendrickson, 2007). Recent evidence suggests that in eukaryotes the primary NEF that interacts with Hsp70 is Hsp110 (Lui & Hendrickson, 2007).

The reaction cycle of Hsp70 begins with recognition of exposed hydrophobic residues on a target substrate, typically performed by Hsp40. However, assistance by Hsp40 is not required for Hsp70 interaction with target proteins. An ATP-Hsp70 complex will then bind to the target protein via several hydrophobic patches in the SBD. The γ-phosphate of ATP transferred to Hsp70, which causes a significant conformational change that "locks" Hsp70 to the target protein, thus preventing initial or further aggregation (Goloubinoff & De Los Rios, 2007). The ADP-Hsp70 complex is considered the active state of Hsp70 and possesses high affinity for the substrate (Hendrickson & Liu, 2008). Hsp110 mediates the release of ADP from cytosolic Hsp70, which results in release of the substrate (Lui & Hendrickson, 2007; Goloubinoff & De Los Rios, 2007).

Protection of SERCA by Hsps.

The mechanisms associated with Hsp70's role in cyto-protection have yet to be fully elucidated. It has been demonstrated in yeast that overexpression of Hsp60 increased cell survivability and reduced protein oxidation after exposure to H_2O_2 (Cabiscol et al., 2002). Another study found that the prokaryote analog of Hsp60, GroEL was able to protect SERCA1a function from thermal inactivation by preventing protein aggregation (Javed et al.,

1999). An *in vitro* study in which isolated SR from rat fast-twitch skeletal muscle was incubated at 37^{o}C or 41^{o}C in the absence or presence of rat recombinant Hsp70, found that at 37^{o}C Hsp70 prevented thermal inactivation of SERCA1a (Tupling et al., 2004). The mechanism associated with Hsp70 protection of SERCA1a activity appeared to be related to preservation of the structural integrity of the N-domain, as indicated by FITC binding assays. Furthermore, 3-D modeling of SERCA1a and Hsp70 suggested that the likely binding region of Hsp70 is at or near the N-domain of SERCA1a.

Recently, it has been demonstrated that co-expression of Hsp70 with SERCA2a in HEK-293 cells protected Ca^{2+}-ATPase activity following exposure to thermal stress (Fu & Tupling, 2007). Similar to the study by Tupling and co-workers (2004), thermal inactivation of SERCA2a was associated with reduced FITC binding, which was prevented in the presence of Hsp70 overexpression (Fu & Tupling, unpublished results). In addition, Hsp70 lowered the degree of oxidation of SERCA2a as demonstrated by a reduction in reactive carbonyl content. In both studies, co-immunoprecipitation assays demonstrated that Hsp70 can physically interact with both SERCA1a (Tupling et al., 2004) and SERCA2a (Fu & Tupling, unpublished results). Taken together, Hsp70 appears to be a strong candidate for protection of SERCA1a and SERCA2a from *in vitro* and *in vivo* thermal stress.

To date, studies have only examined the protective effects of Hsps on SERCAs following thermal stress. It should be noted that thermal stress *in vivo* increases ROS production. Indeed $O_2^{\bullet -}$ production increases as a function of temperature from 37 to 45^{o}C (Salo et al., 1991). Moreover, during muscle contraction, IR and certain diseases the generation of ROS/RNS are exacerbated (Kobzik et al., 1994; Zweier 1988; Ying et al., 2008). A consequence of ROS/RNS production during these conditions is an inactivation of

SERCA (Matsunaga et al., 2003; Tupling et al., 2001; Ying et al., 2008). Preconditioning enhances Hsp70 levels in the myocardium and protects contractile function and preserves SR Ca^{2+} handling (O'Brien et al., 1997). This suggests that Hsp70 may protect SERCA2a function during ischemia and the subsequent reperfusion (i.e. oxidative stress). However, no study has examined the interaction between Hsp70 and SERCA2a using direct incubation with ROS/RNS. Therefore, it is important to characterize the isolated effects of ROS/RNS on the physical interaction between SERCA2a and Hsp70.

Purpose.

The purpose of this study is to determine the effects of $ONOO^-$ on SERCA2a structure and function in the presence and absence of Hsp70 overexpression. The major objectives are:

(1) to determine if Hsp70 can prevent $ONOO^-$-induced inactivation of SERCA2a and

(2) to determine the mechanisms associated with $ONOO^-$-induced inactivation of SERCA2a.

(3) to determine the molecular mechanisms responsible for protection (or lack there of) of SERCA2a by Hsp70.

HEK-293 cells co-transfected with SERCA2a and pMT2 (empty vector) or with SERCA2a and Hsp70 cDNAs were exposed to $ONOO^-$ chronically (multiple micro additions), similar to the methods of Gutiérrez-Martin et al. (2004). SERCA2a aggregation, FITC binding, reactive carbonyl content and tyrosine nitration were assessed using immunoprecipitation and Western blotting techniques to determine the mechanisms associated with inactivation and potential protection by Hsp70.

Hypotheses.

It was hypothesized that:

(i) $ONOO^-$ would reduce Ca^{2+}-ATPase activity of SERCA2a and that the overexpression of Hsp70 would fully protect activity.

(ii) overexpression of Hsp70 would prevent 3-nitrotyrosine formation on SERCA2a following $ONOO^-$ exposure.

(iii) $ONOO^-$ would cause a reduction in FITC binding to SERCA2a and overexpression of Hsp70 would protect the N-domain of SERCA2a and preserve FITC binding.

(iv) $ONOO^-$ would increase reactive carbonyl content on SERCA2a, which would be attenuated in the presence of Hsp70 overexpression.

Methods

Materials.

To synthesize $ONOO^-$, isopentyl nitrite and 30% H_2O_2 were purchased from Sigma. The protein-G-sepharose used to immunoprecipitate SERCA2a was purchased from Sigma. Pyruvate kinase, NADH and the Complete® protease inhibitor were from Roche. The SERCA2a antibody was purchased from Affinity BioReagents; Anti-nitrotyrosine antibody was from Cayman Chemicals; Anti-Hsp70 was from Assay Designs; Anti-fluoroscein/Oregon Green® was from Invitrogen; Anti-DNP was from Sigma and all secondary antibodies were from Santa Cruz. All other reagents were purchased from Bioshop Canada, Sigma or Fisher and were of analytical grade.

Synthesis of $ONOO^-$.

$ONOO^-$ was synthesized similar to the protocol developed by Uppu & Pryor (1996). In an ice-water bath, 1.56 M H_2O_2, 1.56 M NaOH, 1.56 mM EDTA in at total volume of 6.94 mL was mixed vigorously with a magnetic stir bar for 10 min. The mixture was removed from the ice-water bath, 5860 μL of 96% isopentyl nitrite was added to the solution, which brought the final volume to 12.8 mL and then the reaction was allowed to proceed at room temperature for 3 hours. Immediately after the 3 hr incubation, two post-processing steps were performed to remove contaminants. First, the mixture was washed 3 times with 2 volumes of dichloromethane to remove any remaining isopentyl nitrite or isopentyl alcohol. Second, the solution was purged with N_2 to remove any dissolved gases or trace organic solvents (Uppu, 2006). To determine the concentration of $ONOO^-$ produced, the $ONOO^-$ solution was diluted 1:1000 and the absorbance was measured at 302 nm (DU 800, Beckman

Coulter). The concentration of $ONOO^-$ was calculated using the extinction coefficient 1670 $M^{-1} \cdot cm^{-1}$ and ranged from 235-270 mM. Aliquots of $ONOO^-$ were stored at -80°C and the concentration was calculated daily prior to use.

Culture and Transfection of HEK-293 Cells.

Human embryonic kidney cells (HEK-293) were cultured in DMEM-high glucose medium (HyClone) supplemented with 10% fetal bovine serum (Sigma), 1% penicillin/streptomycin (Sigma) and 2 mM L-Glutamine (HyClone) and housed in a humidified incubator at 37°C with 5% CO_2. When HEK-293 cells neared confluence they were split at a ratio of 1:15 and transferred to 150 x 20 mm plates (Falcon). Twenty-four hours later the medium was aspirated and replaced with 18 mL of fresh media. Cells were then co-transfected with plasmids encoding rabbit SERCA2a (Brandl et al., 1986; Asahi et al., 1999) in combination with the pMT2 vector (S2a-pMT2) or with human Hsp70 (S2a-Hsp70) (Wu et al., 1985) using the Ca^{2+}-phosphate precipitation method (Asahi et al., 1999; Kimura et al., 1998; Odermatt et al., 1998). Prior to experiments with $ONOO^-$, the transfection ratio of SERCA2a and Hsp70 cDNA was determined such that the expression of SERCA2a was optimized (3 μg : 1 μg).

Experimental Design.

On a given day, cells were split into two groups and co-transfected with S2a-pMT2 or S2a-Hsp70. Seventy-two hours after co-transfection, each group was subdivided such that half the S2a-pMT2 and S2a-Hsp70 served as controls (i.e. were not exposed to $ONOO^-$) and the other half of the cells were exposed to $ONOO^-$. Therefore, a total of 4 groups were

created (i.e. Control S2a-pMT2, S2a-Hsp70 and $ONOO^-$ S2a-pMT2, S2a-Hsp70). In the $ONOO^-$ groups, repeated micro volumes of $ONOO^-$ were added directly to cells in culture. During chronic exposure to $ONOO^-$ a total of 10 pulses of 250 μM $ONOO^-$ was added each min for a total incubation time of 10 min. The final concentration of $ONOO^-$ in culture was 2.5 mM. To account for changes in pH due to the basic solution used to stabilize $ONOO^-$, periodic additions of a 1M stock solution of HEPES were added to maintain the pH in a range of 7.2-7.6. The effect of $ONOO^-$ on the pH of the media was determined prior to work with cultured cells using a 3-point calibrated pH meter (Fisher) by adding $ONOO^-$ to complete media and monitoring the changes in pH. The volume of 1M HEPES required to maintain the pH in the 7.2-7.6 range was then determined and did not exceed 25 mM in culture.

Isolation of the microsomal fraction.

Immediately following exposure to $ONOO^-$ the culture medium was removed from all groups and the cells were resuspended in ~24 mL of 1X phosphate buffered saline (PBS) with 5 mM EDTA. Cells were centrifuged for 5 min at 1300 g (SA 600 Rotor, Sorvall) and washed twice with 5 mL of ice-cold homogenizing buffer containing 250 mM sucrose, 5 mM HEPES, pH 7.5, 10 mM NaN3, and 0.2 mM PMSF. The final pellet was homogenized in 1500 μL of homogenizing buffer using a handheld glass homogenizer (Duall 20, Kontes). Next, homogenates were sonicated (Vibra Cell, Sonics & Materials) for a total of 20 sec with a duty cycle of 2 sec on and 5 sec off at 60% intensity. A small aliquot of homogenate was flash frozen in liquid nitrogen for determination of Hsp70 expression in the S2a-pMT2 and S2a-Hsp70 groups and the remaining sample was used to isolate the microsomal fraction.

Briefly, the homogenate was centrifuged at 9265 g for 30 min (SA 600, Sorval) to remove the heavy membrane fraction. The supernatant was transferred to clean tubes and spun at 171500 g for 60 min (70.1 Ti Rotor, Beckman). The resulting pellet was resuspended in 400 µL homogenizing buffer, aliquots were flash frozen in liquid nitrogen and stored at -70^{o}C until subsequent analysis.

Ca^{2+}- dependent Ca^{2+}-ATPase activity.

Measurements of Ca^{2+}-dependent Ca^{2+}-ATPase activity were made at 37^{o}C using a spectrophotometric assay developed by Simonides and Van Hardeveld (1990) adapted to a 96-well plate reader (Duhamel et al., 2007). The assay buffer contained (in mM) 20 HEPES, pH 7.0, 100 KCl, 10 $MgC1_2$, 1 EGTA, 10 NaN_3, and 10 PEP. For each sample, a cocktail containing 5 mM ATP, 18 U/mL LDH, 18 U/mL PK, 1 µM Ca^{2+} ionophore A23187, 200 µL microsomes and 3.6 mL assay buffer was combined in a test tube on ice. The cocktail was then subdivided (300 µL) into 16 microcentrifuge tubes with varying concentrations of $CaCl_2$. The $[Ca^{2+}]_f$ corresponding to each $CaCl_2$ addition was assessed separately, on different microsome aliquots, by use of dual-wavelength spectrofluorometry and the Ca^{2+}-fluorescent dye Indo-1. The range of calcium additions translates into a *p*Ca range of ~7.0-5.0. Next, two 100 µL aliquots from each of the sixteen 300 µL subdivisions were loaded onto a clear bottom 96-well plate. The final step was the addition of ~2 µL of 33 mM NADH to each well. ATPase activity represents the decrease in NADH absorbance at 340 nm (SPECTRAmax Plus, Molecular Devices). To distinguish Ca^{2+}-ATPase activity from background ATPase activity, 240 µM of the specific SERCA inhibitor, cyclopiazonic acid (CPA) was used (Seidler et al., 1989). The difference between the total activity and the basal

activity (activity in the presence of CPA) represented the Ca^{2+}-ATPase activity. The reaction proceeded for 60 min at 37^{o}C and the rate of decline in NADH absorbance was recorded approximately half way through the incubation period when the signals were linear (R^2 > 0.9). All values were normalized to total protein concentration and SERCA2a expression as determined by the Lowry assay and Western blotting, respectively. The V_{max} was taken as the peak rate of activity, which typically occurred between a pCa of 5.5-5.0.

Western blot analysis.

Western blotting was performed to determine the relative expression levels of SERCA2a and Hsp70 in microsomes and homogenate prepared from S2a-pMT2 and S2a-Hsp70. The linearity of band density was determined for each transfected batch of cells. For SERCA2a and Hsp70 respectively, a total of 4 and 0.33 μg of total protein was loaded on 7.5% polyacrylamide gels and separated using standard SDS-PAGE protocols (Laemmli, 1970). The gels were cut where appropriate and the proteins were transferred to a polyvinyldiene difluoride (PVDF) membrane (Bio-Rad) and blocked for 1 hr at room temperature with 10% milk in Tris-buffered saline plus Tween (TBS-T; Tris-HCl, pH 7.5, 150 mM NaCl, 0.1% Tween 20). After blocking, antibodies for SERCA2a (1:4000; MA3-919, Affinity BioReagents) and Hsp70 (1:1000; SPA-810, Assay Designs) were applied for 1 hr at room temperature and overnight at 4^{o}C, respectively. Subsequently, membranes were washed with TBS-T for 30 min and probed for 1 hr with horse-radish peroxidase conjugated anti-mouse secondary antibody (1:2000, Santa Cruz). After washing with TBS-T, the images were visualized using an enhanced chemiluminescent kit (GE Healthcare) and a bio-imaging system. Images were captured and analyzed using the software GeneSnap and GeneTools,

respectively (Syngene). The group which contained the highest SERCA2a content (i.e. largest optical density) was assigned a value of 1 and the optical densities from the other 3 groups were normalized to that optical density. These correction factor for SERCA2a content were then used to normalize V_{max}, FITC binding, 3-nitrotyrosine and reactive carbonyl content.

In a subset of Western blots, SERCA2a content was determined in the absence of 2-mercaptoethanol (i.e. under non-reducing conditions). Under these conditions it is presumed that RSSR bonds formed during treatment with ROS/RNS remain intact. Therefore, any protein aggregates will not migrate as far as the monomer band during SDS-PAGE. These aggregate proteins will appear as higher molecular weight bands in the Western blot. Microsomes from S2a-pMT2 and S2a-Hsp70 were blotted for SERCA2a under non-reducing conditions and then normalized to SERCA2a content from blots performed under reducing conditions.

Co-immunoprecipitation of SERCA2a and Hsp70.

To determine if $ONOO^-$ can induce Hsp70 binding to SERCA2a, co-immunoprecipitation of SERCA2a using anti-hsp70 antibody (SPA-810; Assay Designs) was performed. Microsomes were diluted to 0.5 mg/mL with H_2O, homogenizing buffer and 2X co-IP buffer (40 mM HEPES, pH 7.5, 300mM NaCl, 2mM EDTA, 10 mM $MgCl_2$, 4 mM PMSF and 1% Tween). The solution was vortexed and centrifuged for 30 min at 16000 g (F2402 Rotor, Beckman GS-15R). The supernatant was transferred to new tubes, combined with 30 μL of a 50% slurry of protein-G-sepharose (v/v in 1X PBS containing 0.1% BSA & 0.01% NaN_3) and rotated for 30 min at 4^{o}C. The protein-G slurry was pelleted and the

supernatants were transferred to new tubes. Next, 1.75 µL of 10% BSA and 1 µg of anti-Hsp70 antibody were added to each tube and the samples were allowed to mix for 55 min at 4^{o}C. The samples were then spun at 12868 g for 10 min and the supernatants were placed in new tubes. Again, 30 µL of the protein-G-sepharose slurry were added to each sample and rotated for 30 min at 4^{o}C. At this point the slurry was pelleted and the supernatant was discarded. The remaining protein-G-sepharose-antibody complex was washed 3 times with 1 mL of 1X co-IP buffer and once with wash buffer (25 mM Tris pH 7.2, 150 mM NaCl). Samples were eluted with 36 µL of elution buffer (100 mM Glycine, pH 2.8) for 15 min on ice. Next, the slurry was pelleted and the supernatant was placed in a new tube containing 2 µL of 1 M Tris, pH 9.0. Finally, 9 µL of 5X sample buffer (123.8 mM Tris pH 6.8, 10% SDS, 50% glycerol, 0.25% bromophenol blue & 25% 2-mercaptoethanol) were added to all samples, which were then separated using SDS-PAGE and probed via Western blotting using anti-SERCA2a antibody.

Isolation of SERCA2a from the microsomes by immunoprecipitation (IP).

It was necessary to immunoprecipitate SERCA2a from the microsomal fraction in order to measure 3-NY content, FITC binding capacity and reactive carbonyl content of SERCA2a. This protocol was followed because in HEK-293 cells there is a large abundance of the Na^{+}/K^{+}-ATPase. The Ca^{2+}-ATPase and the Na^{+}/K^{+}-ATPase are members of the P-type transporter family and are of similar size (~100 kDa) and 3-D structure (Morth et al., 2007; Toyoshima, 2000). Therefore, it would be impossible to discern the Ca^{2+}-ATPase band from the Na^{+}/K^{+}-ATPase band when blotting for 3-NY content, FITC or reactive carbonyl content. In addition, by immunoprecipitating SERCA2a the sample becomes concentrated with

SERCA2a, which improves the ability to a) detect 3-NY, FITC and reactive carbonyls and to b) detect differences between groups. Therefore, for each of these protocols (i.e. 3-NY content, FITC, carbonyl), SERCA2a was first immunoprecipitated from the microsomes.

SERCA2a nitrotyrosine content.

The degree of nitrosylation of SERCA2a was determined using the methods of Li et al. (2006) with slight modifications. Microsomes (1 mg/mL) were diluted with homogenizing buffer, H_2O and 2X IP buffer (20 mM Tris, pH 7.4, 600 mM Sucrose, 1% CHAPS & 1 protease inhibitor tablet; Complete© Roche) and mixed gently by inversion. The samples were then centrifuged for 10 min at 6000 g at 4^{o}C. The supernatants were transferred to new tubes and 4 µL of 50% BSA and 1 µg of anti-SERCA2a antibody were added to each tube. The samples were allowed to mix overnight at 4^{o}C. The next morning 5 µL of a 50% protein-G-sepharose slurry was added to each sample and rotated at 4^{o}C for 2 hrs. The protein-G-sepharose was then centrifuged and the supernatant was discarded. The sepharose beads were then washed 3 times with 1X IP buffer. After washing, 10 µL of 2X sample buffer was added to each tube. Subsequently, 2 µL of each sample was loaded onto a 7.5% polyacrylamide gel in duplicate and separated by standard SDS-PAGE protocols. The membrane was probed with a monoclonal primary antibody specific for nitrotyrosine residues (1:1500, Cayman Chemicals). After washing with TBS-T the membrane was incubated with goat anti-mouse secondary antibodies (1:2000, Santa Cruz) and visualized using an ECL kit (GE HealthCare). The duplicate sample was probed for SERCA2a content using anti-SERCA2a antibody and was used to normalize the nitrotyrosine content for each sample.

Fluoroscein isothiocyanate binding capacity.

FITC binding to SERCA2a was assessed on microsomes isolated from all groups of cells. In this instance SERCA2a was IP using a non-denaturing lysis buffer. This was important because it preserved the tertiary structure of SERCA2a. After washing, samples were eluted on ice for 15 min with 15 μL of elution buffer. Subsequently, 5 μL of 1.0 M Tris pH 9.0 was added to each sample and the sepharose was mixed thoroughly. Immediate neutralization of the sample was critical because this ensured that the 3-D structure and more specifically the N-domain of SERCA2a was not altered by the acidic pH of the elution buffer. After neutralization, the sepharose beads were centrifuged and 10 μL of the supernatant were combined with 80 μL of FITC binding buffer (50 mM Tris-HCl, pH 8.8, 250 mM sucrose, 0.1 mM $CaCl_2$, 5 mM $MgCl_2$, 20 μM FITC & protease inhibitors) and incubated at room temperature in the dark for 1 hour. To stop the reaction, 20 μL of 5X sample buffer were added to each sample. Next, 10 μL of each sample were loaded on a 7.5% polyacrylamide gel and separated by SDS-PAGE. The membranes were probed with anti-fluoroscein/Oregon Green® monoclonal antibody (4-4-20, Invitrogen) diluted 1:5000 in 5% milk in TBS-T. Lastly, the membranes were probed with the appropriate secondary antibodies and the images were developed using GeneSnap (Syngene). The optical density was normalized to the content of SERCA2a in each group.

SERCA2a reactive carbonyl content.

Oxidation of SERCA2a protein was assessed by measuring the reactive carbonyl content of SERCA2a that had been immunoprecipitated from microsomes derived from cells treated with or without $ONOO^-$. Samples were immunoprecipitated using a protocol identical

to that used for nitrotyrosine determination. After washing the sepharose beads, samples were solubilized by adding 10 μL of 5% SDS to each tube. At this point 9 μL of the solution was removed, combined with 9 μL of 2X sample buffer and used for determination of SERCA2a content via Western blotting. Next, 12 μL of 10 mM 2,4-dinitrophenylhydrazine (DNPH) in 2 M HCl was added to the remaining sample, which were then incubated at room temperature for 15 min. Immediately after incubation with 2,4-DNPH, 12 μL of neutralization buffer (2 M Tris & 30% glycerol) were added to each tube, which were then placed back on ice. Subsequently, 18 μL of 2X sample buffer was added to each tube. Finally, 30 μL of 4X stacking buffer were added to each tube. The samples were centrifuged for 2 min and 10 μL of the supernatant were applied to a 7.5% gel and separated by SDS-PAGE. The proteins were transferred to a PVDF membrane and blocked over night with 10% BSA in TBS-T. After washing with TBS-T for ~10 min, the membrane was incubated for 1 hr at room temperature with a mouse monoclonal antibody specific for DNP (SPE-7, Sigma) that was diluted 1:20000 in TBS-T supplemented with 0.2% BSA. After washing, the membrane was probed with an anti-mouse secondary antibody (Santa Cruz) diluted 1:5000 and the signal was visualized using an ECL Plus kit (GE Healthcare) and the GeneSnap software package.

Data Analysis.

Data presented below was collected from three independent experiments and are expressed as means ± standard error of the mean (SE). When an identical trend (i.e. increase or decrease compared to S2a-pMT2) was observed in all three trials it was considered an effect.

Results

Overexpression of Hsp70 in HEK-293 cells.

To optimize the expression of SERCA2a in HEK-293 cells co-transfected with SERCA2a and Hsp70 cDNAs, a transfection ratio of 3 μg SERCA2a cDNA:1 μg Hsp70 cDNA was utilized. This transfection ratio resulted in a ~1.9-fold increase in the expression of Hsp70 in the S2a-Hsp70 cells when compared to endogenous Hsp70 present in S2a-pMT2 cells (Figure 3).

Ca^{2+}-dependent Ca^{2+}-ATPase activity.

The Ca^{2+} dependence of Ca^{2+}-ATPase activity was determined in microsomes collected from control or $ONOO^-$ treated HEK-293 cells co-transfected with S2a-pMT2 or S2a-Hsp70. Figure 4 illustrates the maximal enzyme activity among each group. Co-transfection of SERCA2a and Hsp70 cDNAs had no effect on V_{max} when compared to SERCA2a alone (Figure 4, left panel). Repeated additions of 250 μM $ONOO^-$ resulted in a ~20% reduction in V_{max} in the S2a-pMT2 group when compared to the control S2a-pMT2 group. However, overexpression of Hsp70 in HEK-293 cells fully protected against $ONOO^-$-induced inactivation of SERCA2a (Figure 4, right panel).

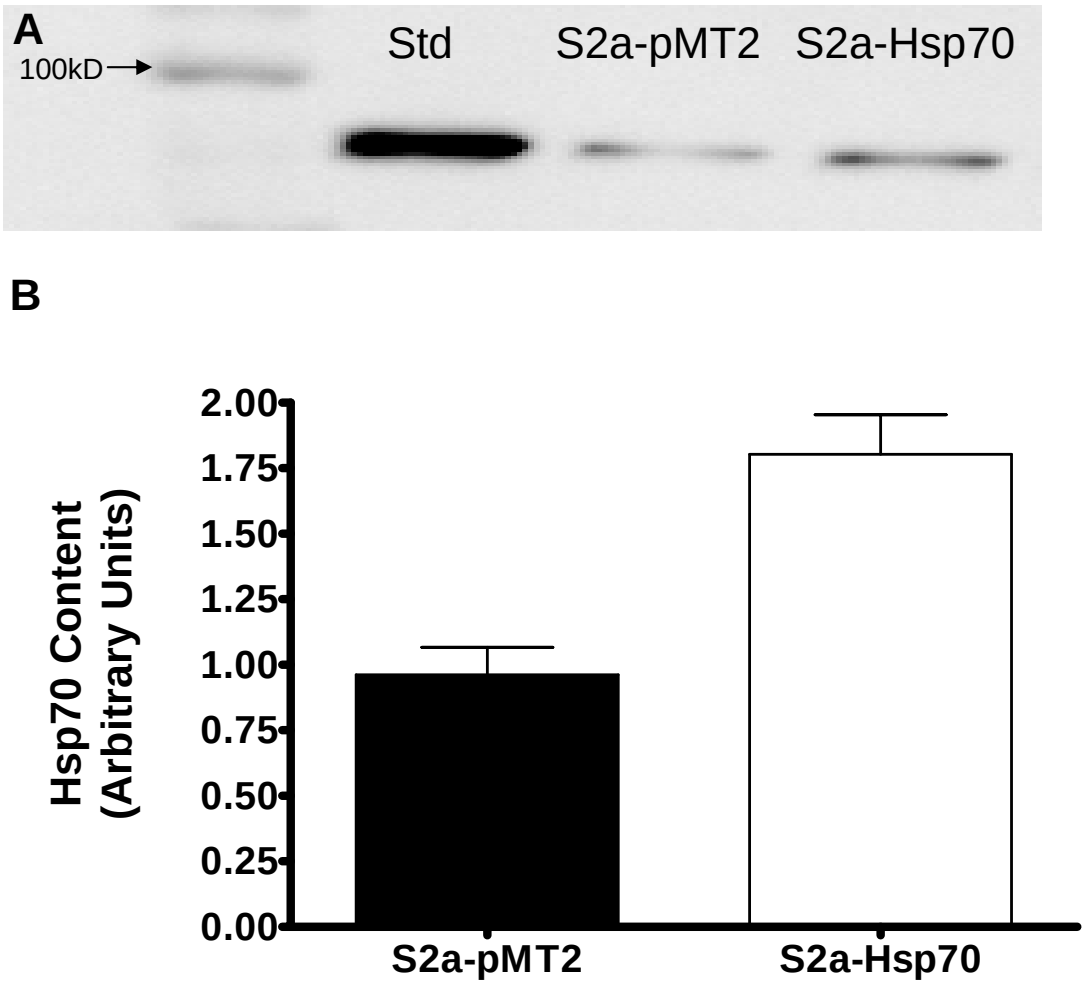

Figure 3: Expression of Hsp70 in S2a-pMT2 and S2a-Hsp70 co-transfected HEK-293 cells. (A) Representative Western blot of Hsp70 protein. Whole cell lysates were separated by SDS-PAGE and Western blotting was performed with a monoclonal antibody for Hsp70 (SPA-810, Assay Designs). The left lane is the molecular weight standard (Western C^{TM}, BioRad). 12.5 ng of recombinant rat Hsp70 protein were used as a positive control (2nd lane, Std). (B) Graphical representation of the optical density of Hsp70 from both groups (*n*=3).

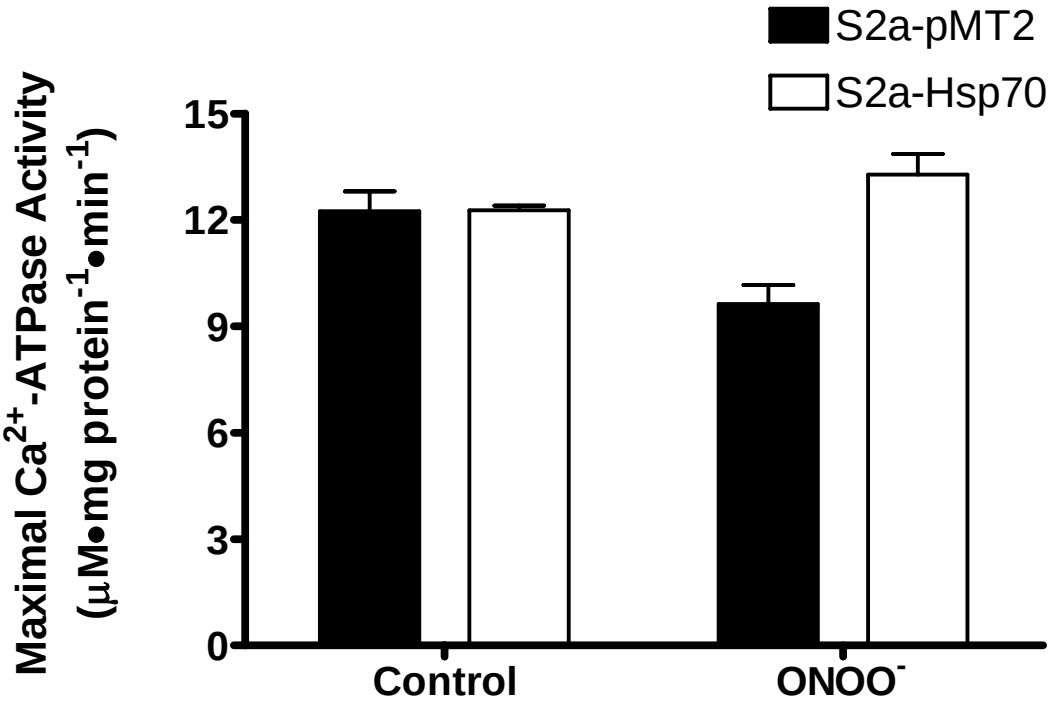

Figure 4: Maximal Ca^{2+}-ATPase activity of SERCA2a. HEK-293 cells were co-transfected with S2a-pMT2 or S2a-Hsp70 cDNAs. Control samples were harvested in the absence of $ONOO^-$. Cells were exposed to micro additions of $ONOO^-$ for a total of 10 min resulting in a final $ONOO^-$ concentration of 2.5 mM (see "Methods" for details). Values are normalized to SERCA2a content and are mean ± SE (*n*=3).

Co-immunoprecipitation.

Once it was determined that overexpression of Hsp70 could protect SERCA2a activity from exposure to $ONOO^-$, it was then necessary to establish whether Hsp70 could physically interact with SERCA2a. To do this, co-immunoprecipitation experiments were performed using microsomes from control and $ONOO^-$ treated cells. Figure 5A depicts a representative Western blot using monoclonal antibodies against SERCA2a. It is evident that Hsp70 and SERCA2a physically interact under all conditions. The Western blot in Figure 5B confirms that Hsp70 was successfully immunoprecipitated by its monoclonal antibody.

Immunoprecipitation and Western blot results.

To determine the mechanisms responsible for Hsp70 protecting SERCA2a activity from nitrosative stress, IP and Western blotting techniques were used to measure FITC binding, 3-nitrotyrosine and reactive carbonyl content as well as aggregation of SERCA2a.

SERCA2a aggregation.

Representative Western blots of SERCA2a from identical groups performed under reducing and non-reducing conditions are shown in Figure 6. Non-reducing Western blots (i.e. absence of 2-mercaptoethanol) were used to detect the presence of high molecular weight aggregates that formed during $ONOO^-$ treatment. Figure 6C is a graphical representation of the optical densities of the distinct (Figure 6B; white arrow) high molecular weight aggregates normalized to SERCA2a content under reducing conditions. In control cells, overexpression of Hsp70 resulted in a ~44% reduction in the appearance of SERCA2a aggregates, which had no influence on V_{max} of SERCA2a. Treatment with $ONOO^-$ resulted in a ~44% increase in SERCA2a aggregation in the S2a-pMT2 when compared to the control

S2a-pMT2 group. When compared to the control S2a-pMT2 group, $ONOO^-$ increased aggregation by ~30% in the S2a-Hsp70 group. However, SERCA2a aggregation was still ~40% lower in the S2a-Hsp70 group compared to S2a-pMT2 following $ONOO^-$ treatment (Figure 6C).

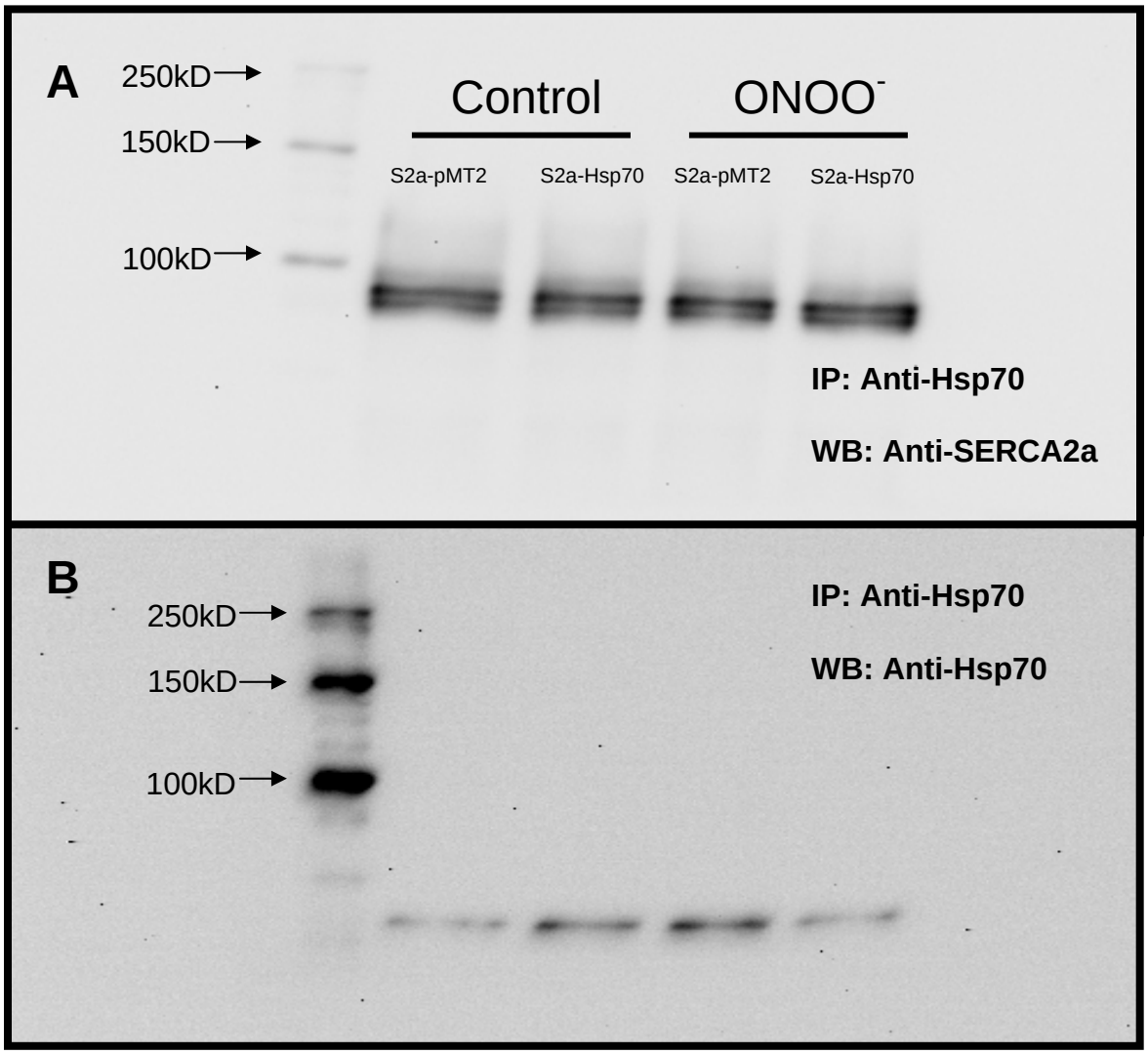

Figure 5: Co-immunoprecipitation of SERCA2a and Hsp70. Microsomes from control and $ONOO^-$ treated HEK-293 cells were used for co-immunoprecipitation using a monoclonal antibody for Hsp70 (SPA-810, Assay Designs) as described under "Methods". (A) The presence of SERCA2a bound to Hsp70 was determined via Western blotting using a monoclonal antibody for SERCA2a (MA3-919, Affinity BioReagents). (B) Detection of Hsp70 in the immuno-complex was also performed by Western blotting using the Hsp70 antibody. Left lane, molecular weight standard (Western C^{TM}, BioRad).

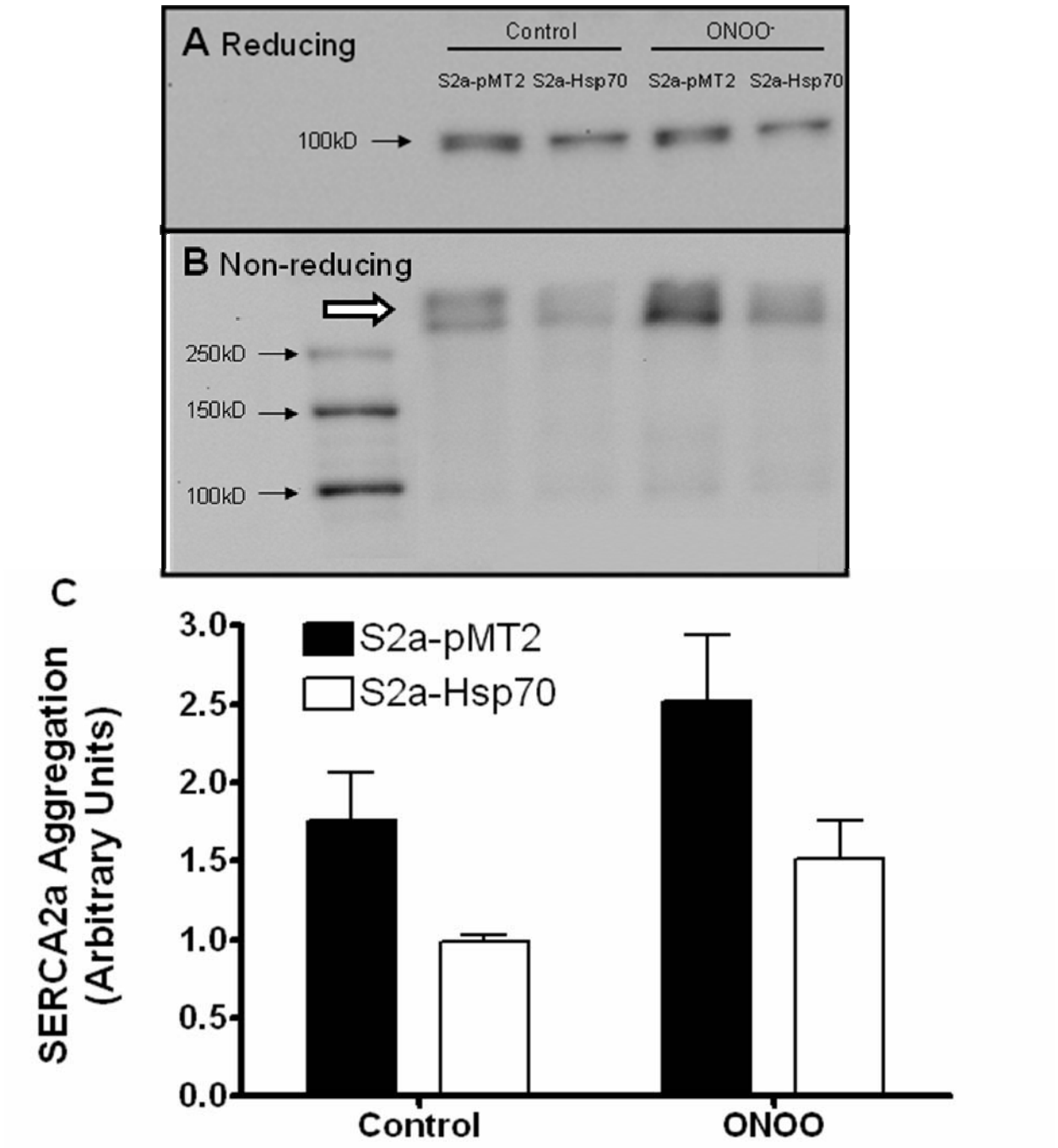

Figure 6: Western blot analysis of SERCA2a high molecular weight aggregates. (A) Representative blot of SERCA2a under *reducing* conditions. The loading sequence is indicated with the appropriate labels. (B) Representative blot of SERCA2a under *non-reducing* conditions. The white arrow indicates high molecular weight aggregates of SERCA2a. (C) Graphical representation of the optical density of the high molecular weight aggregates normalized to SERCA2a content under *reducing* conditions (*n*=3).

SERCA2a nitrosylation.

In order to isolate SERCA2a from the microsomal fraction, IP was performed. Once isolated, the extent of nitrosylation on SERCA2a was determined using an antibody specific for 3-NY residues. Western blot analysis revealed no differences between control S2a-pMT2 and S2a-Hsp70 groups when normalized to SERCA2a content (Figure 7). Contrary to the initial hypothesis, treatment with $ONOO^-$ did not alter 3-NY content on SERCA2a in the S2a-pMT2 or S2a-Hsp70 groups.

FITC binding capacity of SERCA2a.

To assess FITC binding capacity of SERCA2a, IP was performed under non-denaturing conditions. Figure 8 indicates that FITC binding was not different between the control S2a-pMT2 and S2a-Hsp70 groups when normalized to SERCA2a content. Unexpectedly, no change in FITC binding capacity of SERCA2a was observed in any group following $ONOO^-$ treatment.

Reactive carbonyl content on SERCA2a.

Lastly, IP and Western blotting were utilized to determine changes in reactive carbonyl content (a measure of protein oxidation) on SERCA2a following exposure to $ONOO^-$. An example of a typical Western blot of reactive carbonyl groups is illustrated in Figure 9A. Upon further examination of optical density (normalized to SERCA2a content), no differences in reactive carbonyl content were observed in the control groups (Figure 9B). However, reactive carbonyl content increased by ~80% in the S2a-pMT2 group following

$ONOO^-$ treatment. Overexpression of Hsp70 completely prevented the oxidation of SERCA2a induced by $ONOO^-$.

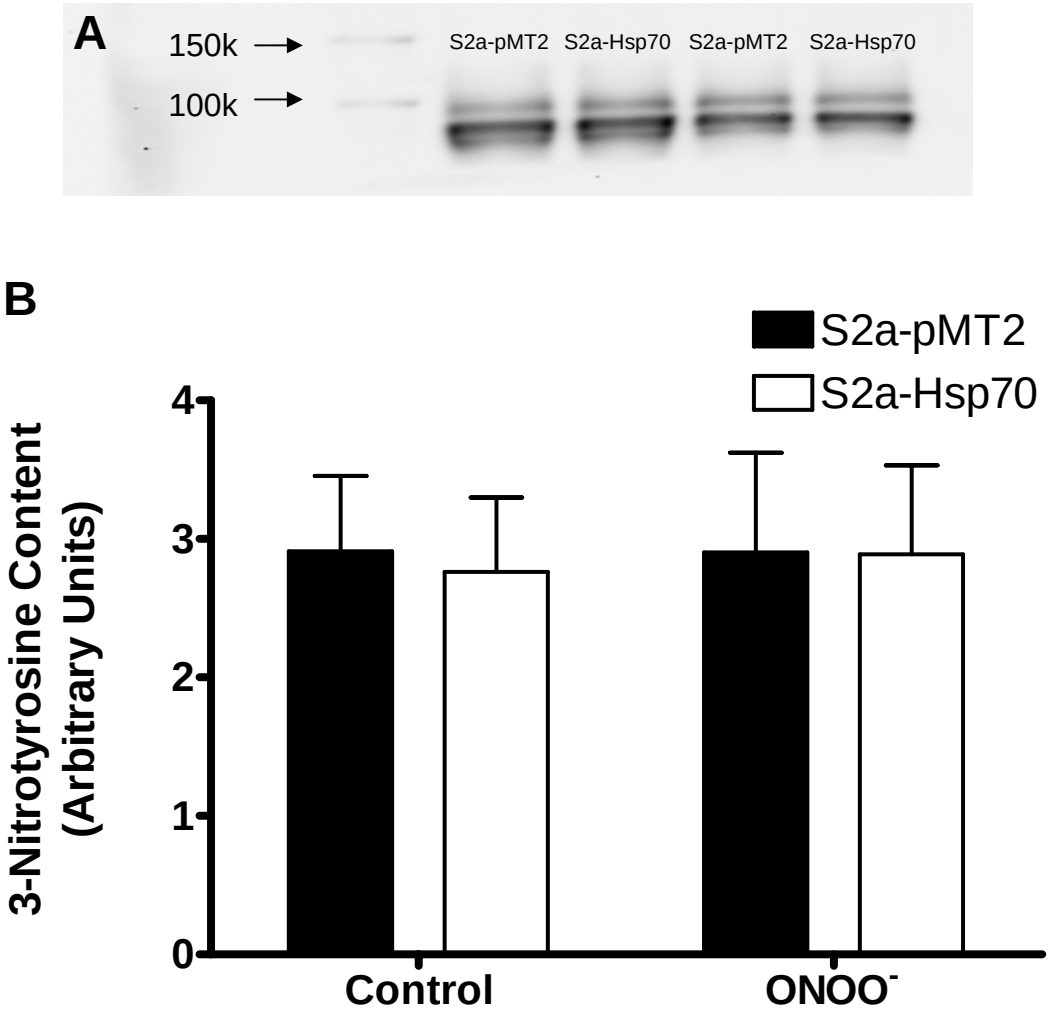

Figure 7: 3-nitrotyrosine levels on SERCA2a. SERCA2a was immunoprecipitated from Control and $ONOO^-$ treated microsomes from S2a-pMT2 and S2a-Hsp70 co-transfected HEK-293 cells as described under "Methods". (A) A representative Western blot of 3-NY content on SERCA2a using a monoclonal antibody specific for 3-NY residues (Cayman Chemicals). (B) Graph of the optical density of Western blots for 3-nitrotyrosine content on SERCA2a (*n*=3). Values were normalized to SERCA2a content in each group.

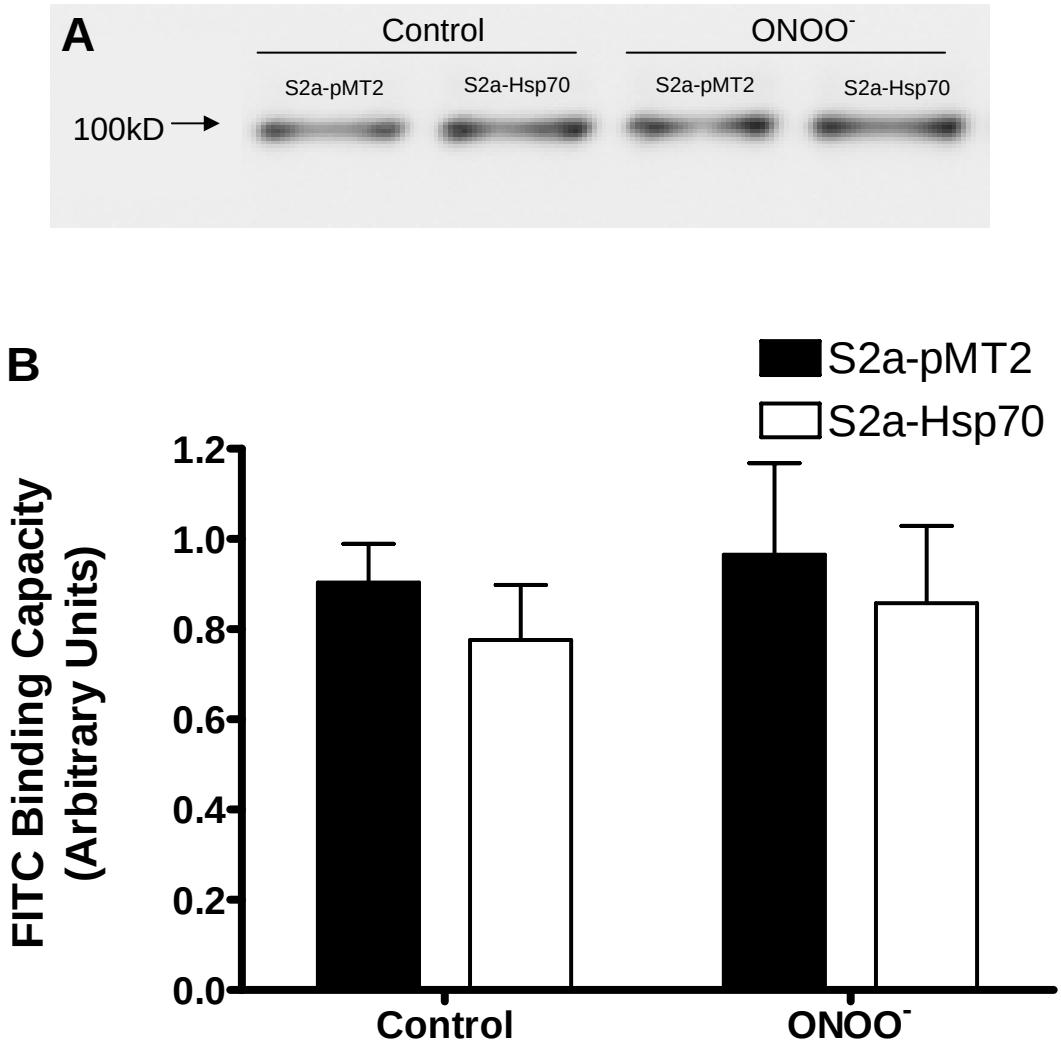

Figure 8: FITC binding capacity of SERCA2a. SERCA2a was immunoprecipitated from Control and $ONOO^-$ treated microsomes from S2a-pMT2 and S2a-Hsp70 co-transfected HEK-293 cells and probed with FITC as described under "Methods". (A) A representative Western blot of FITC bound to SERCA2a determined via an anti-fluoroscein monoclonal antibody (4-4-20, Invitrogen). (B) The optical density of FITC binding to SERCA2a was normalized to SERCA2a content from samples run on a separate gel (n=3).

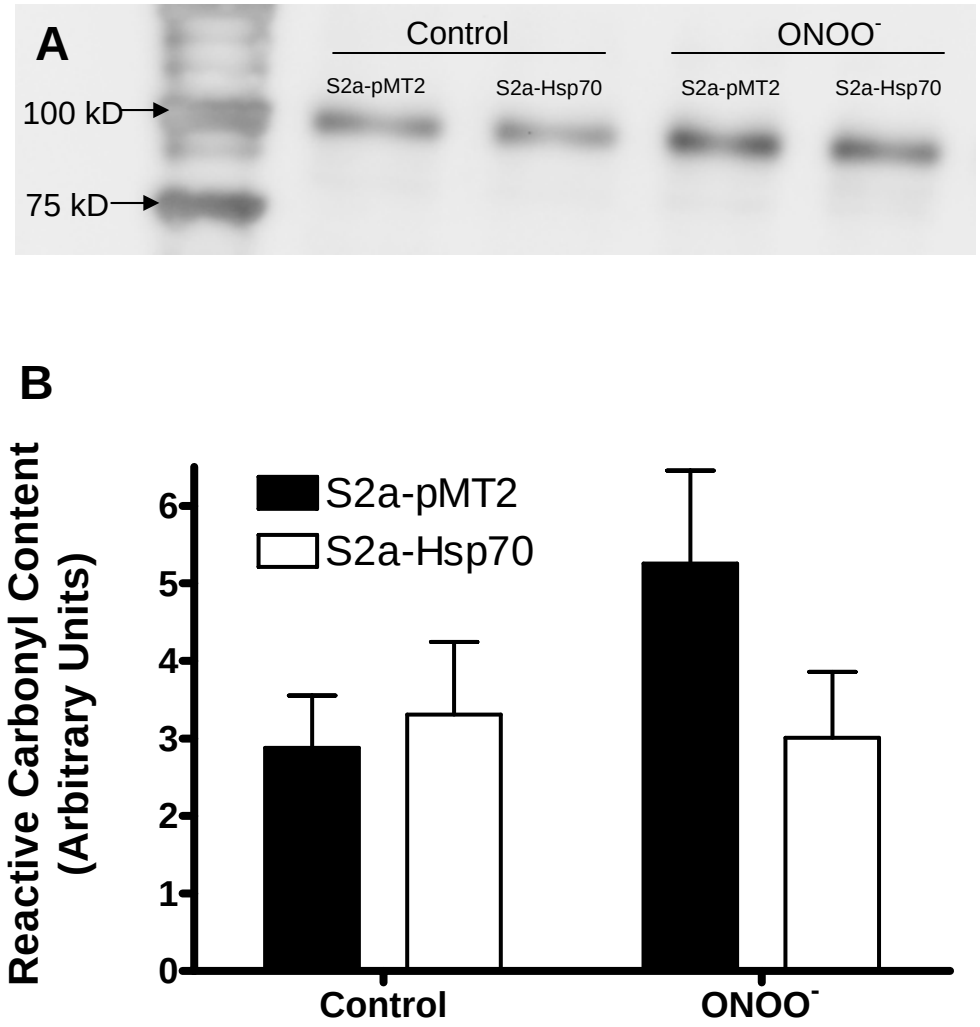

Figure 9: Reactive carbonyl content on SERCA2a. SERCA2a was immunoprecipitated from microsomes and probed for reactive carbonyl groups as outlined in "Methods". (A) A representative Western blot probed with monoclonal anti-DNP (Sigma). (B) A graph of the optical density of reactive carbonyls normalized to SERCA2a content determined separately on a different gel (*n*=3).

Discussion

Overexpression of Hsp70.

This study utilized HEK-293 cells as a vessel for the overexpression of SERCA2a and Hsp70 in order to determine whether Hsp70 can protect SERCA2a structure and function from exposure to $ONOO^-$. Co-transfection with S2a-Hsp70 cDNAs resulted in a ~1.9-fold increase in the Hsp70 protein in whole cell lysates when compared to S2a-pMT2 cell lysates. This level of Hsp70 overexpression is similar in magnitude with previous studies in humans and rodents that utilized various modalities to induce a stress response. A study by Milne and Noble (2002), demonstrated that treadmill running (33 m/min for 1 h) in rats resulted in a ~5-, 2.5- and 6-fold increase in Hsp70 protein in cardiac, red vastus and white vastus muscles, respectively. In the absence of contractile activity, simply raising the core temperature of rats to 42^oC for 15 min increased the Hsp70 content in cardiac muscle by ~35% (Ruell et al., 2004). A recent study that used exercise as a mode to induce Hsp70 found that 30 min of intermittent isometric knee extension exercise resulted in ~40% increase in Hsp70 protein (Tupling et al., 2007). Other human studies that have utilized exercise to induce Hsp70 have found increases in Hsp70 protein ranging from ~170-3000% (Khassaf et al., 2001; Thompson et al., 2001; Thompson et al., 2003; Morton et al., 2006). It is evident that the ~1.9-fold overexpression of Hsp70 measured in this study is well within the physiological induction range of both rodents and humans.

Influence of $ONOO^-$ and Hsp70 on SERCA2a activity.

Incubation of S2a-pMT2 HEK-293 cells with 2.5 mM $ONOO^-$ resulted in a ~20% reduction in V_{max}. These results are in agreement with the hypothesis that incubation with $ONOO^-$ would reduce SERCA2a activity. Numerous *in vitro* studies have examined the effects of ROS/RNS on SERCA function. Incubation of enriched SR fractions with either $NO^{\cdot}$, $^{\cdot}OH$, HOCl, $FeSO_4$/EDTA, H_2O_2 or $ONOO^-$ had detrimental effects on the ATPase activity of SERCA (Kaplan et al., 2003; Ishii et al., 1998; Xu et al., 1997; Favero et al., 1998; Grover et al., 1992; Gutiérrez-Martin et al., 2004). A study by Viner and co-workers (1999b) compared the effects of $ONOO^-$ on enriched SR from young rat fast- and slow-twitch muscles. This study demonstrated that incubation with 100 μM $ONOO^-$ decreased Ca^{2+}-ATPase activity in fast and slow SR by ~30 and 13%, respectively (Viner et al., 1999b). The differences in susceptibility of SERCA1a and SERCA2a to $ONOO^-$ were ascribed to differences in the degree of Tyr and Cys modification on each isoform. It appears as though specific ROS/RNS (i.e. $ONOO^-$) can interact with SERCA1a or SERCA2a in very distinct ways. Incubation of SERCA1a with $ONOO^-$ only results in significant nitrosylation of Tyr122 (Sharov et al., 2002). Conversely, Tyr753, Tyr294 and Tyr295 are readily nitrated on SERCA2a following exposure to $ONOO^-$ (Knyushko et al., 2005). With ageing, SERCA2a is preferentially nitrosylated, whereas SERCA1a undergoes primarily Cys oxidation (Knyushko et al., 2005; Sharov et al., 2006). Further isoform differences were noted by Grover and colleagues (1997), who observed that the inactivation of SERCA2b caused by H_2O_2 was greater than the H_2O_2-induced inactivation of SERCA3. These authors attributed this to the fact that the amino acid sequence of SERCA2b contains 4 more Cys residues when compared to the sequence of SERCA3.

A study found that when SR from fast-twitch skeletal muscle was exposed chronically to $ONOO^-$ (final [$ONOO^-$]: 250 μM) that Ca^{2+}-ATPase activity was reduced by ~80% (Gutiérrez-Martin et al., 2004). Interestingly, when an acute bolus of 250 μM $ONOO^-$ was combined with enriched SR, Ca^{2+}-ATPase activity was only reduced by ~50%. The large discrepancy in reduction in Ca^{2+}-ATPase activity in the current study (~20%) compared to that of Gutiérrez-Martin and co-workers (2004) (~80%) is likely due to differences in SERCA isoform and methodological differences. Studies by Gutiérrez-Martin and co-workers (2004) and Sharov and others (2006) observed large decreases in enzyme activity when SERCA1a was incubated with $ONOO^-$. The current study utilized a $ONOO^-$ concentration ten times stronger than that of Gutiérrez-Martin et al. (2004). It may seem puzzling that the reduction in activity was a modest 20%. However, it should be noted that the incubation time in this thesis was short (10 min) when compared to Gutiérrez-Martin and co-workers (2004), which was upwards of 50 minutes. Furthermore, cells were incubated in culture with $ONOO^-$ versus *in vitro* incubation (Gutiérrez-Martin et al., 2004). When ROS/RNS are incubated with SR fractions *in vitro* the molarity of ROS/RNS added to the assay buffer is the concentration that interacts with SERCA. However, it is likely that the actual concentration of $ONOO^-$ that reached the ER membrane within the HEK-293 cells, and thus interacted with SERCA2a, was far less than the micro bolus of 250 μM added each minute. This is because $ONOO^-$ would have needed to first diffuse throughout the culture media, cross the plasma membrane and then diffuse within the cytosol to the site of SERCA2a expression. In addition, the degradation of $ONOO^-$ occurs rapidly at physiological temperatures, which further limits $ONOO^-$ ability to react with SERCA2a at the ER membrane (Denicola et al., 1998). Taken together, it is plausible that the $ONOO^-$

concentration that reacted with SERCA2a was far less than that added to the culture dish, which most likely explains the modest (~20%) reduction in SERCA2a activity. A similar reduction in SERCA2a activity of 13% was found following incubation of enriched SR from slow-twitch skeletal muscle with 100 μM $ONOO^-$ (Viner et al., 1999b). Perhaps the concentration of $ONOO^-$ that reacted with SERCA2a in the present study was closer in magnitude to that used in the study by Viner and co-workers (1999b). Regardless, this study demonstrates that incubation of cells in culture with $ONOO^-$ can inactivate proteins within those cells.

The overexpression of Hsp70 in the present study had no effect on the V_{max} of SERCA2a under control conditions. The most novel and exciting finding in the current study was that physiological overexpression of Hsp70 fully protected SERCA2a function from exposure to $ONOO^-$. Numerous studies have shown that anti-oxidants or reducing agents may fully or partially protect SERCA function. However, this is the first study to demonstrate that a molecular chaperone, Hsp70, can protect SERCA2a activity in living cells that are exposed to exogenous $ONOO^-$. In fact, only a handful of studies have been published that examined the interaction between Hsp70 and SERCA. An *in vitro* study by Javed and co-workers (1999) found that the prokaryote analog of Hsp60, GroEL, protected SERCA1a from thermal inactivation by preventing protein aggregation. More recently, it was demonstrated that when enriched SR membranes isolated from rat fast-twitch skeletal muscle were incubated at 37°C for 30 min that there was a ~20% reduction in SERCA1a V_{max} (Tupling et al., 2004). However, when recombinant rat Hsp70 was added to the enriched SR fraction under identical heat stress conditions, V_{max} of SERCA1a was fully protected. These results are very similar with those of the current study. The current study found that

incubation with $ONOO^-$ also reduced Ca^{2+}-ATPase activity by ~20%. However, overexpression of Hsp70 fully protected SERCA2a from $ONOO^-$-induced inactivation. Interestingly, in the study by Tupling et al. (2004), when thermal stress was prolonged (i.e. >60 min) or samples were incubated at 41°C, Hsp70 was not able to protect SERCA1a function. There appears to be a limit to the extent to which Hsp70 can protect SERCA1a from heat stress (Tupling et al., 2004). Perhaps, if the $ONOO^-$ concentration or incubation time were increased then a further reduction in SERCA2a activity would occur. Given the similar magnitude of inactivation of SERCA in the current study and in the study by Tupling and colleagues (2004), there is likely a threshold where Hsp70's ability to protect SERCA2a from $ONOO^-$-induced inactivation is abolished. Therefore, further investigation into the ability of Hsp70 to protect against severe oxidative stress is warranted.

Further adding to the knowledge of SERCA and Hsp70 interaction is a study by Fu & Tupling (2007) that co-transfected HEK-293 cells with S2a-pMT2 and S2a-Hsp70 and then subjected the cells to heat stress. In the S2a-pMT2 cells, heat shock at 40°C for 1 h resulted in a ~60% reduction in V_{max} of SERCA2a. However, V_{max} of SERCA2a was fully protected in S2a-Hsp70 cells. In the study by Fu & Tupling (2007), inactivation of SERCA2a may have been the result of direct attack by ROS/RNS, thermal denaturation or both. In that study the production of ROS/RNS during heat stress was not assessed. The elevated temperature (40°C) would likely have resulted in an increased production of $O_2^{\cdot-}$ (Salo et al., 1991). Both Tupling et al. (2004) and Fu & Tupling (unpublished results) found that thermal stress reduced FITC binding to SERCA consistent with observations from several other studies (Xu et al., 1997; Favero et al., 1998). However, the current study failed to observe any changes in FITC binding in any groups. This suggests that different mechanisms lead to the inactivation

of SERCA2a in the current study compared to the studies by Tupling et al. (2004) and Fu & Tupling (unpublished results). This highlights the importance of characterizing the effects of specific ROS and RNS on the interaction between Hsp70 and SERCA2a.

Immunoprecipitation of SERCA2a.

To determine the amount of 3-NY, FITC binding and reactive carbonyls on SERCA2a, it was necessary to immunoprecipitate SERCA2a from the mircosomal fraction. This was an important step because SERCA2a was transfected into HEK-293 cells. Not surprisingly, these kidney cells contain significant amounts of the α_1-subunit of the Na^+/K^+-ATPase. The Ca^{2+}-ATPase and the Na^+/K^+-ATPase are members of the P-type pump family and share functional and structural similarities. Both pumps bind their respective cations within their transmembrane domains and harness the energy from aspartylphosphate formation to transport the cations across their particular membranes. The α_1-subunit of the Na^+/K^+-ATPase and the Ca^{2+}-ATPase are ~100 kDa and thus migrate identically when applied to SDS-PAGE. In addition, these two pumps possess a similar 3-D structure (Morth et al., 2007; Toyoshima, 2000). Similar to SERCA, FITC labels Lys501 in the N-Domain of the α_1-subunit of the Na^+/K^+-ATPase (Farley et al., 1984). Given the homology between these two pumps, it is highly probable that the Na^+/K^+-ATPase present in the HEK-293 cells may have been nitrosylated and/or oxidized following the $ONOO^-$ treatment. Clearly, if the whole microsomal fraction was separated by SDS-PAGE and probed for either FITC, 3-NY or reactive carbonyl groups, then it would have been impossible to discern whether the signal originated from Ca^{2+}-ATPases or Na^+/K^+-ATPases.

A secondary benefit of immunoprecipitating SERCA2a is that very little of the final immunoprecipitate was required to detect strong Western blot signals. In other words, the sample had been concentrated, which helped to improve detection of bands associated with FITC, 3-NY and reactive carbonyls on SERCA2a. Therefore, to determine the mechanisms responsible for $ONOO^-$ induced inactivation of SERCA2a and how overexpression of Hsp70 protected SERCA2a function IP and several Western blotting techniques were employed.

Assessment of 3-nitrotyrosine content on SERCA2a.

It was hypothesized that $ONOO^-$ would increase 3-NY content in S2a-pMT2 cells. However, treatment of S2a-pMT2 HEK-293 cells with $ONOO^-$ did not increase 3-NY content on SERCA2a compared to the control S2a-pMT2 group. Furthermore, the overexpression of Hsp70 under control and $ONOO^-$ conditions had no effect on 3-NY content. Several studies have demonstrated that incubation of SERCA with $ONOO^-$ results in significant increases in 3-NY content (Gutiérrez-Martin et al., 2004; Viner et al., 1999b; Sharov et al., 2002). One study incubated SERCA1a with 0.1 and 0.25 mM $ONOO^-$ and observed a robust band at ~100 kDa when proteins were blotted for 3-NY content (Gutiérrez-Martin et al., 2004). Such intense staining for 3-NY content on SERCA1a is surprising considering SERCA1a's apparent resistance to nitrosylation when compared to SERCA2a (Sharov et al., 2002; Knyushko et al., 2005). Indeed, SERCA2a is more readily nitrosylated *in vivo* during biological ageing or *in vitro* following exposure to $ONOO^-$ (Viner et al., 1999b; Knyushko et al., 2005).

There are several possible explanations as to why 3-NY content was not altered following exposure to $ONOO^-$. There is a possibility that the technique employed was not

sensitive enough to detect differences in 3-NY content. First, SERCA2a was immunoprecipitated and then blotted for 3-NY using an antibody specific for 3-NY residues. It is not known whether multiple antibodies can recognize multiple 3-NY residues on a single peptide or if only a single antibody can recognize one of many 3-NY residues on a single peptide. If the later is true, then it is not surprising that 3-NY content on SERCA2a did not change, since there appears to be a basal level of SERCA2a nitrosylation (Knyushko et al., 2005).

In young rats there is very little 3-NY residues detectable on SERCA2a (Tyr753) from skeletal muscle. However, in young cardiac muscle there are several nitrated Tyr residues (Tyr122, 130, 497, 586 & 990) (Knyushko et al., 2005). In aged rats the only significant increase in Tyr nitration occurs at the vicinal tyrosines, Tyr294 & Tyr295. These Tyr residues are in close proximity to the Ca^{2+} binding sites of SERCA2a and modification to these residues are believed to contribute to the reduction in Ca^{2+}-ATPase activity observed with ageing (Knyushko et al., 2005). Selective nitrosylation of Tyr294 and Tyr295 would have been better detected using an antibody specifically designed to detect the nitration of these Tyr residues on SERCA2a (Xu et al., 2006). An even more sensitive measure of 3-NY formation on SERCAs requires the use of HPLC-tandem mass spectroscopy (Viner et al., 2000; Sharov et al., 2006). This technique can not only determine the specific amino acids modified, but it can also determine the type of adduct formed on the amino acid residues (e.g. NO_2-, GSS-, SNO-, etc.) (Adachi et al., 2004; Knyushko et al., 2005). The formation of 3-NY may have taken place, but these tyrosine residues could have been further oxidized into tyrosyl radicals and then into bityrosines (Alvarez & Radi, 2003). This may explain the development of high molecular weight aggregates of SERCA2a that were observed following

treatment with $ONOO^-$. However, it is more likely that oxidation of amino acids (e.g. Cys) occurred before a substantial amount of 3-NY residues could accumulate. This is because only a single monomer band was present when SERCA2a was detected under reducing Western blot conditions. If SERCA2a formed bityrosines for example, reducing agents would not have been able to dissolve the SERCA2a aggregates and a high molecular weight band would have appeared on the Western blot (Viner et al., 1997). Also, it has been suggested that high concentrations of $ONOO^-$ are required to elicit significant nitrosylation of tyrosines (Denicola et al., 1998).

Structural integrity of the N-domain as indicated by FITC binding to SERCA2a.

It was hypothesized that incubation of S2a-pMT2 HEK-293 cells with 2.5 mM $ONOO^-$ would have reduced FITC binding to SERCA2a and that FITC binding would have been preserved in S2a-Hsp70 cells. However, no differences in FITC binding in either control or $ONOO^-$ treated groups were found. These results were surprising considering the evidence that suggests *in vitro* incubation of SERCA1a with ROS compromises the structural integrity of the N-domain. One study found that when SR isolated from fast-twitch skeletal muscle was incubated with HOCl that there was a concentration dependent decrease in Ca^{2+}-ATPase activity (Favero et al., 1998). This study also demonstrated that there was a HOCl concentration dependent decrease in the capacity of FITC to bind to SERCA1a, suggesting an association between the structural integrity of the N-domain and the ATPase activity of SERCA1a. An elegant study by Xu and colleagues (1997) demonstrated that pre-incubation of cardiac and skeletal SR with 1 mM ATP fully protected Ca^{2+}-ATPase activity from $^{\cdot}OH$ induced inactivation. These authors suggested that when ATP occupies the nucleotide

binding pocket within the N-domain that $^{\cdot}OH$ is prevented from interacting with critical amino acids (i.e. Cys349) within that region and thus enzyme function is preserved. A study that measured FITC binding to SERCA1a demonstrated that heat shock of enriched SR at 37^{o}C resulted in a time-dependent reduction in the structural integrity of the N-domain (Tupling et al., 2004). A novel aspect of that study was that incubation with recombinant rat Hsp70 fully protected the N-domain for up to 60 min of heat stress. Similarly, FITC binding was reduced significantly in S2a-pMT2 HEK-293 cells following heat shock at 40^{o}C for 1 hr (Fu & Tupling, unpublished results). However, when S2a-Hsp70 were expressed together, FITC labeling of SERCA2a was fully protected following heat stress. Modeling of SERCA1a and Hsp70 indicated that Hsp70 interacts with SERCA1a at or near the N-domain (Tupling et al., 2004). The current study was performed in living cells, in the presence of endogenous ATP and Hsp70, which may have been sufficient to prevent $ONOO^{-}$-induced damage to the N-domain of SERCA2a. These findings are unique compared with other studies and suggest that both $ONOO^{-}$-induced inactivation of SERCA2a and protection of SERCA2a by Hsp70 can occur in the absence of structural modifications to the N-domain. This suggests that $ONOO^{-}$ modified amino acids in either the transmembrane, P- and/or A-domain and that Hsp70 can physically interact with SERCA2a in these regions.

Hsp70 prevents oxidation of SERCA2a by $ONOO^{-}$.

It is possible that $ONOO^{-}$ interacted with SERCA2a in an area other than the N-domain, such that FITC binding was not affected. The likelihood that amino acids were oxidized some distance from Lys514 (FITC binding site) is supported by the reactive carbonyl data. This study demonstrated that incubation with $ONOO^{-}$ increased the amount of

reactive carbonyl groups (indication of protein oxidation) on SERCA2a by ~80%. The elevation in reactive carbonyl groups was completely abolished when Hsp70 was overexpressed in HEK-293 cells.

Substantial evidence suggests that one of the primary mechanisms responsible for ROS/RNS induced inactivation of SERCA is protein oxidation. In particular oxidation of Cys residues on SERCA have been shown to associate with a reduction in enzyme activity (Favero et al., 1998; Scherer & Deamer, 1986; Kaplan et al., 2003). However, other studies have demonstrated that Cys oxidation was only partly responsible for the reduction in Ca^{2+}-ATPase activity (Viner et al., 1997; Gutiérrez-Martin et al., 2004). The oxidation of Cys residues is quite complex and can lead to several end products (e.g. Sulfenic acid, sulfinic acid, sulfonic acid, etc.) with a Cys RSSR bond being the most well observed end product (Alvarez & Radi, 2003).

Site specific modification of oxidation of Cys on SERCA by ROS/RNS.

Structural analysis of SERCA following exposure to ROS/RNS suggests that multiple Cys residues are oxidized depending on the assay conditions and that certain Cys residues may act as intrinsic antioxidants protecting other amino acids that are crucial for SERCA function (Viner et al., 2000; Sharov et al., 2006). A study by Viner et al. (1999a) found that low concentrations of $ONOO^-$ modified five Cys residues in a near 1:1 stoichiometry with the observed reduction in SERCA1a Ca^{2+}-ATPase activity. Incubation with higher concentrations of $ONOO^-$ caused a ~40% loss in ATPase activity, which only correlated well with the modification of Cys344 and Cys349. These amino acids are proximal to Asp351 and thus the creation of a RSSR bond between them would presumably hinder catalytic activity

of SERCA. Indeed, the proximity between Cys344 and Cys349; Cys670, Cys674 and Cys675 or Cys876 and Cys888 makes them potential targets for RSSR formation (Viner et al., 2000). When SERCA1a was incubated with $NO^{\cdot}$, $ONOO^{-}$ or amino acid peroxides, it was demonstrated that the most highly oxidized Cys residues were Cys268, 349, 364, 471, 670, 674, 675, 774 & 938 (Viner et al., 2000; Sharov et al., 2006; Dremina et al., 2007). From these Cys residues, only Cys471 is located within the N-domain sequence (Viner et al., 2000; MacLennan et al., 1985). Cys670, 674 and 675 are located within the hinge domain between the N-domain and M5. However, Cys674 and Cys675 are <12 Å away from Asp351, thus oxidation and formation of a RSSR bond between these residues could hinder aspartylphosphate formation (Sharov et al., 2006). Interestingly, Cys 268, 744 and 938 are located within M3, M5 and M9, respectively (Dremina et al., 2007). Oxidation of these Cys residues may influence the protein-lipid dynamics of SERCA with its surrounding membrane.

Although Cys oxidation and SH content were not explicitly measured in the current study, it seems reasonable to speculate that some degree of the oxidation of SERCA2a was directed at Cys residues. Numerous studies have indicated that $ONOO^{-}$ reduced the number of free SH groups on SERCA (Gutiérrez-Martin et al., 2004; Sharov et al., 2006). Quite often the reduction of free thiols on SERCA is associated with the appearance of high molecular weight aggregates of SERCA. Studies have shown that $ONOO^{-}$, diamide and AAPH reduced the amount of SH groups and increased the amount of high molecular weight aggregates of SERCA in a concentration- or time-dependent manner (Viner et al., 1999; Viner et al., 1997; Senisterra et al., 1997). Under control conditions, overexpression of Hsp70 reduced SERCA2a aggregation, which did not influence V_{max} of SERCA2a when compared to S2a-

pMT2. However, SERCA2a aggregation increased in the S2a-pMT2 group following incubation with $ONOO^-$, which was accompanied by a reduction in V_{max}. Interestingly, $ONOO^-$ caused aggregation of SERCA2a in the S2a-Hsp70 group but to a lesser extent than the S2a-pMT2 group. These data suggest that lowering SERCA2a aggregation may not influence V_{max} but if aggregation increases past a threshold then inactivation of SERCA2a occurs. This could explain, in part, the mechanism by which Hsp70 protected SERCA2a function.

Potential mechanisms of Hsp70 protecting SERCA2a function.

Several possible scenarios may explain how overexpression of Hsp70 preserved SERCA2a ATPase activity following exposure to $ONOO^-$. The first is that Hsp70 may have buffered some of the nitrosative stress by reacting with $ONOO^-$. When Hsp60 expression was knocked down in yeast, exposure to H_2O_2 increased reactive carbonyl content on several proteins, including Hsp60 (Cabiscol et al., 2002). Furthermore, incubation of GroEL with $ONOO^-$ significantly reduced its refolding activity. The main amino acid target on GroEL was oxidation of Met residues to methionine sulfoxide (Khor et al., 2004). Therefore, the possibility that $ONOO^-$ oxidized Hsp70 in the current study cannot be ruled out.

The co-immunoprecipitation and Western blot data suggest that Hsp70 protected SERCA2a activity through a physical interaction that prevented oxidation and limited aggregation. In S2a-pMT2 cells, $ONOO^-$ increased the oxidation of SERCA2a by ~80%. This likely caused a conformational change in SERCA2a 3-D structure, which exposed hydrophobic amino acids to the cytosolic milieu (Senisterra et al., 1997). Detection of these hydrophobic residues by Hsp40, which is present in HEK-293 cells, would direct Hsp70 to

bind to SERCA2a (Kumar & Mitra, 2005). At this point Hsp70 could have "held" SERCA2a without refolding it such that SERCA2a would not aggregate with other oxidized proteins (Mayer & Bukau, 2005), or Hsp70 would have refolded the partially denatured SERCA2a and restored its function.

An alternative mechanism would involve SERCA2a forming inactive aggregates. Oxidation of SERCA2a increased the appearance of high molecular weight aggregates in the S2a-pMT2 group. Protein aggregates are toxic to the cell and are repaired quickly by molecular chaperones such as Hsp70 (Saibil, 2008). When Hsp70 was overexpressed in HEK-293 cells, exposure to $ONOO^-$ increased aggregation of SERCA2a. Presumably, this aggregation was detected by Hsp70 (or perhaps even Hsp40), which resulted in the recruitment of Hsp70 to disaggregate SERCA2a. Once bound to SERCA2a, Hsp70 would proceed through its reaction cycle changing its conformation in order to refold and/or pry apart SERCA2a. This process requires repeated cycles of Hsp70 binding to the substrate, hydrolysis of ATP, conformational changes within Hsp70's tertiary structure and release of substrate from Hsp70 (Goloubinoff & De Los Rios, 2007).

Model of the potential interaction sites between SERCA2a and Hsp70.

The arguments presented above support the hypothesis that $ONOO^-$ oxidized amino acid residues in a region other than the N-domain. Potential candidates are, Tyr294, 295 and 753, as well as Cys674, 675 and 938 to name a few (Knyushko et al., 2005; Sharov et al., 2006). Modeling of the potential interaction sites between SERCA1a and Hsp70 has been performed (Tupling et al., 2004). The SERCA1a-Hsp70 interactions predicted by Tupling et al. (2004) as well as potential interaction sites between SERCA2a-Hsp70 induced by $ONOO^-$

are illustrated in Figure 10. Interestingly, one of the most stable conformations of SERCA1a and Hsp70 had Hsp70 located juxtapose to the N-domain (Tupling et al., 2004). The middle image in Figure 10A is most intriguing, as it places Hsp70 in a region encompassing parts of the P-domain, A-domain and stalk region. This binding conformation is in accord with studies that suggest that Cys349 is a crucial amino acid with respect to SERCA catalytic activity (Xu et al., 1997; Viner et al., 2000). Also, Cys670, 674 and 675 have been shown to be modified by RNS and are in proximity to this proposed binding conformation of SERCA1 and Hsp70 (Viner et al., 2000; Sharov et al., 2006). Other amino acids of interest are Tyr294, Ty295 and Cys938. These residues are intimate with the Ca^{2+} binding pocket and the protein-lipid interface, respectively. Perhaps Hsp70 can interact with SERCA2a at the protein-lipid interface or even traverse the ER membrane to interact with luminal amino acids. Recent evidence suggests that Hsp70 can physically interact with acidic glycolipids and phospholipids (Harada et al., 2007). Furthermore, Hsp70 has been shown to insert in the plasma membrane of cells following cellular stress (Vega et al., 2008). A hypothetical interaction between SERCA2a and Hsp70 following $ONOO^-$ treatment is presented in Figure 10.

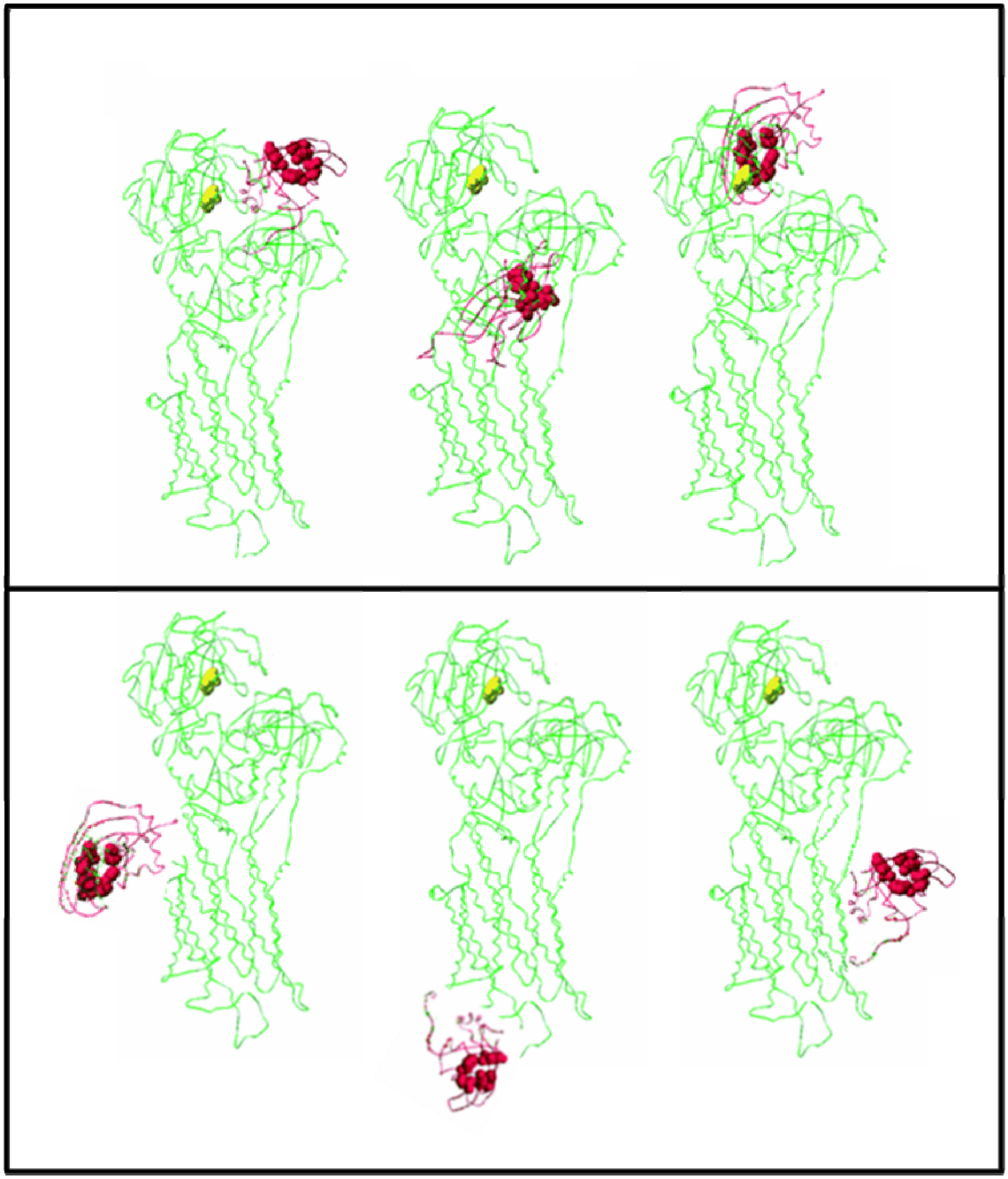

Figure 10: Computer modeled and hypothetical interaction sites between SERCA1a and Hsp70. The upper panel depicts the most stable binding conformations of SERCA1a and Hsp70 determined by Tupling et al. *J. Biol. Chem*. 279(50): 52382-52389, 2004. The green ribbon is SERCA1a in the E2 conformation. The red ribbon and balls represent the substrate binding domain of bovine heat shock protein cognate and the Hsp70 binding site, respectively. The FITC binding site of SERCA1a (Lys515) is illustrated by the yellow balls. The lower panel depicts hypothetical binding of Hsp70 to SERCA2a (SERCA1a 3-D structure used) near the transmembrane domains (left and right images) or near the vicinal Tyr residues, Tyr294 and Tyr295 (middle image).

Physiological relevance of Hsp70 protecting SERCA2a.

Disruption in Ca^{2+} homeostasis is a functional consequence of exercise, ageing, certain disease states and in ischemia-reperfusion (IR). Each of these conditions shares a common thread, and that is the increased production of ROS/RNS (Kobzik et al., 1994; Zweier 1988; Ying et al., 2008). The ability to maintain Ca^{2+} homeostasis (i.e. protect SERCA function) in the face of oxidative stress could conceivably improve performance and/or recovery time or increase cell survivability. The current study sheds light on this issue by providing direct evidence that Hsp70 can preserve SERCA2a catalytic activity following exposure to highly reactive $ONOO^-$.

Summary.

In summary, this is the first study to demonstrate that physiological overexpression of Hsp70 can protect SERCA2a activity from incubation with exogenous $ONOO^-$ in cultured cells. $ONOO^-$ caused a ~20% reduction in SERCA2a Ca^{2+}-ATPase activity, which was completely abrogated by Hsp70 overexpression. SERCA2a co-immunoprecipitated with Hsp70 under all of the experimental conditions in this study. It was hypothesized that $ONOO^-$ would increase 3-NY content and reduce FITC binding in the S2a-pMT2 group and that these structural modifications to SERCA2a would be prevented by Hsp70. However, there were no changes in 3-NY content and FITC binding in any of the four groups. The mechanisms associated with reduced SERCA2a activity were protein oxidation and aggregation. In the S2a-Hsp70 group, SERCA2a aggregation was reduced by ~44% when compared to the S2a-pMT2. When S2a-pMT2 was incubated with $ONOO^-$, SERCA2a aggregation increased by ~44%; however, incubation with $ONOO^-$ only increased SERCA2a

aggregation by ~30% in the S2a-Hsp70 group when compared to S2a-pMT2. Lastly, incubation of S2a-pMT2 cells with $ONOO^-$ caused a ~80% increase in the reactive carbonyl content of SERCA2a. The overexpression of Hsp70 completely prevented $ONOO^-$-induced oxidation of SERCA2a.

Conclusion.

The results of this thesis suggest that Hsp70 can protect SERCA2a from direct exposure to $ONOO^-$ by preventing $ONOO^-$-induced oxidation and aggregation of SERCA2a. This was accomplished through a physical interaction between SERCA2a and Hsp70. Hsp70 likely bound to SERCA2a in a region some distance from the N-domain. In addition, binding of Hsp70 to SERCA2a help to limit the formation of high molecular weight aggregates, which was most likely from oxidation of Cys residues. This is the first study to demonstrate that Hsp70 can protect SERCA2a from direct attack from $ONOO^-$.

Limitations.

Due to the very low Ca^{2+}-ATPase activity in the microsomal fractions, it was very difficult to achieve smooth, sigmoidal Ca^{2+}-ATPase activity curve. That is not to say, however, that a clear Ca^{2+}-dependence of Ca^{2+}-ATPase activity was not observed. Sequential increases in the concentration of Ca^{2+} resulted in a step-wise increase in ATPase activity, which ultimately resulted in a subsequent decline in activity. Since, adequate sigmoidal Ca^{2+}-ATPase curves could not be generated this study was unable to comment or conclude on the effects of $ONOO^-$ on the cooperativity of Ca^{2+} binding to SERCA2a or the sensitivity of SERCA2a to Ca^{2+}.

This study utilized several Western blotting techniques to determine the mechanisms associated with $ONOO^-$-induced inactivation of SERCA2a. Although differences in reactive carbonyl content were observed, perhaps the use of more sensitive techniques (i.e. HPLC-tandem MS) would have improved the understanding of how $ONOO^-$ reacted with SERCA2a in the current study.

Incubation with $ONOO^-$ was performed on living cells in culture. Every attempt was made to ensure that $ONOO^-$ was mixed throughout the entire volume of culture media. However, it is possible that groups of cells were exposed to higher concentrations of $ONOO^-$ compared to others. For example, the area where $ONOO^-$ was injected into culture would experience a sharp spike in the concentration of $ONOO^-$, which may have severely damaged those cells whilst only moderately damaging other cells once $ONOO^-$ was mixed into the media. Furthermore, it is not known what concentration of $ONOO^-$ actually reacted with SERCA2a. It would likely be much less than what was added to the culture media, considering the distance needed for $ONOO^-$ to travel to interact with SERCA2a and the very short half life of $ONOO^-$ under physiological conditions (<0.1 sec).

Future directions.

Future studies will examine isoform differences following incubation with $ONOO^-$. More specifically, a direct comparison between SERCA1a and SERCA2a and the ability of Hsp70 to protect theses proteins from $ONOO^-$-induced inactivation should be examined. It would also be prudent to determine the threshold, if any, where Hsp70 can no longer protect SERCA2a function from increasing concentrations of $ONOO^-$. In addition, the ability of Hsp70 to protect SERCAs from other oxidants (e.g. H_2O_2 or $O_2^{\cdot -}$) should be examined.

Future studies will also look to extend these findings to the whole tissue/organ level. For example, preconditioning the heart with a mild stress results in a substantial increase in Hsp70 protein and provides cellular and functional protection from severe ischemia-reperfusion. The rise in Hsp70 is necessary for cyto-protection following IR. The generation of ROS/RNS during IR would likely have deleterious effects on SERCA2a activity, which could lead to a significant rise in the $[Ca^{2+}]_f$. Calcium overload is a known inducer of apoptosis, which may contribute to the cellular damage and loss of function observed with severe IR. Perhaps Hsp70 can interact with SERCA2a in the preconditioned heart and prevent oxidative inactivation of SERCA2a. This hypothesis is somewhat contentious, as studies have provided evidence for and against this claim. Therefore, further examination of this topic is needed to elucidate the mechanisms by which Hsp70 protects the myocardium from IR injury.

References

Abu-Abed M, Mal TK, Kainosho M, MacLennan DH & Ikura M. Characterization of the ATP-binding domain of the sarco(endo)plasmic reticulum Ca(2+)-ATPase: probing nucleotide binding by multidimensional NMR. *Biochemistry* 41: 1156-1164, 2002.

Adachi T, Weisbrod RM, Pimentel DR, Ying J, Sharov VS, Schöneich C & Cohen RA. S-Glutathiolation by peroxynitrite activates SERCA during arterial relaxation by nitric oxide. *Nat. Med*. 10(11): 1200-1207, 2004.

Alvarez B & Radi R. Peroxynitrite reactivity with amino acids and proteins. *Amino Acids*. 25: 295-311, 2003).

Anthonisen AN, Clausen JD & Andersen JP. Mutational analysis of the conserved TGES loop of sarcoplasmic reticulum Ca2+-ATPase. *J. Biol. Chem*. 281(42): 31572-31582, 2006.

Arruda AP, Oliveira GM, Carvalho DP & de Meis L. Thyroid hormones differentially regulate the distribution of rabbit skeletal muscle Ca^{2+}-ATPase (SERCA) isoforms in light and heavy sarcoplasmic reticulum. *Mol. Membr. Biol.* 22: 529-537, 2005.

Asahi M, Kimura Y, Kurzydlowski K, Tada M & MacLennan DH. Transmembrane helix M6 in sarco(endo)plasmic reticulum Ca(2+)-ATPase forms a functional interaction site with phospholamban. Evidence for physical interactions at other sites. *J. Biol. Chem*. 274(46): 32855-32862, 1999.

Asahi M, Kurzydlowski K, Tada M & MacLennan DH. Sarcolipin inhibits polymerization of phospholamban to induce superinhibition of sarco(endo)plasmic reticulum Ca^{2+}-ATPases (SERCAs). *J. Biol. Chem.* 277: 26725-26728, 2002.

Asahi M, Sugita Y, Kurzydlowski K, De Leon S, Tada M, Toyoshima C & MacLennan DH. Sarcolipin regulates sarco(endo)plasmic reticulum Ca2+-ATPase (SERCA) by binding to transmembrane helices alone or in association with phospholamban. *Proc. Natl. Acad. Sci.* 100(9): 5040-5045, 2003.

Babu GJ, Bhupathy P, Carnes CA, Billman GE & Periasamy M. Differential expression of sarcolipin protein during muscle development and cardiac pathophysiology. *J. Mol. Cell. Cardiol.* 43: 215-222, 2007.

Bhupathy P, Babu GJ & Periasamy M. Sarcolipin and phospholamban as regulators of cardiac sarcoplasmic reticulum Ca2+ ATPase. *J. Mol. Cell. Cardiol*. 42(5): 903-911, 2007.

Brandl CJ, Green NM, Korczak B, & MacLennan DH. Two Ca^{2+} ATPase genes: Homologies and mechanistic implications of deduced amino acid sequences. *Cell* 44: 597-607, 1986.

Burk SE, Lytton J, MacLennan DH, & Shull GE. cDNA cloning, functional expression, and mRNA tissue distribution of a third organellar Ca^{2+} pump. *J. Biol. Chem.* 264: 18561-18568, 1989.

Cabiscol E, Bellí G, Tamarit J, Echave P, Herrero E & Ros J. Mitochondrial Hsp60, resistance to oxidative stress, and the labile iron pool are closely connected in Saccharomyces cerevisiae. *J. Biol. Chem.* 277: 44531-44538, 2002.

Carroll S, Nicotera P & Pette D. Calcium transients in single fibers of low-frequency stimulated fast-twitch muscle of rat. *Am. J. Physiol*. 277(6 Pt 1):C1122-129, 1999.

Castilho RF, Carvalho-Alves PC, Vercesi AE & Ferreira ST. Oxidative damage to sarcoplasmic reticulum Ca^{2+}-pump induced by Fe^{2+}/H_2O_2/ascorbate is not mediated by lipid peroxidation or thiol oxidation and leads to protein fragmentation. *Mol. Cell. Biochem.* 159: 105-114, 1996.

Chin ER, Olson EN, Richardson JA, Yang Q, Humphries C, Shelton JM, Wu H, Zhu W, Bassel-Duby R & Williams RS. A calcineurin-dependent transcriptional pathway controls skeletal muscle fiber type. *Genes Dev*. 12(16): 2499-2509, 1998.

Dally S, Bredoux R, Corvazier E, Andersen JP, Clausen JD, Dode L, Fanchaouy M, Gelebart P, Monceau V, Del Monte F, Gwathmey JK, Hajjar R, Chaabane C, Bobe R, Raies A & Enouf J. Ca2+-ATPases in non-failing and failing heart: evidence for a novel cardiac sarco/endoplasmic reticulum Ca2+-ATPase 2 isoform (SERCA2c). *Biochem. J.* 395 (2): 249-258, 2006.

De Meis L & Sorenson M. ATP regulation of calcium transport in back inhibited sarcoplasmic reticulum. *Biochim. Biophys. Acta* 984: 373-378, 1989.

Denicola A, Souza JM & Radi R. Diffusion of peroxynitrite across erythrocyte membranes. *Proc Natl Acad Sci USA*. 95(7): 3566-3571, 1998.

Dremina ES, Sharov VS, Davies MJ & Schöneich C. Oxidation and inactivation of SERCA by selective reaction of cysteine residues with amino acid peroxides. *Chem. Res. Toxicol*. 20(10): 1462-1469, 2007.

Duhamel TA, Green HJ, Stewart RD, Foley KP, Smith IC & Ouyang J. Muscle metabolic, SR Ca(2+) -cycling responses to prolonged cycling, with and without glucose supplementation. *J. Appl. Physiol*. 103(6): 1986-1998, 2007.

Dux L, Taylor KA, Ting-Beal HP & Martonosi A. Crystallization of the Ca^{2+}-ATPase of sarcoplasmic reticulum by calcium and lanthanide ions. *J. Biol. Chem.* 260(21): 11730-11743, 1985.

Farley RA, Tran CM, Carilli CT, Hawke D & Shively JE. The amino acid sequence of a fluorescein-labeled peptide from the active site of (Na,K)-ATPase. *J. Biol. Chem.* 259: 9532–9535, 1984.

Favero TG, Colter D, Hooper PF & Abramson JJ. Hypochlorous acid inhibits Ca^{2+}-ATPase from skeletal muscle sarcoplasmic reticulum. *J. Appl. Physiol.* 84: 425-430, 1998.

Ferrington DA, Reijneveld JC, Bar PR & Bigelow DJ. Activation of the sarcoplasmic reticulum Ca^{2+}-ATPase induced by exercise. *Biochim. Biophys. Acta.* 1279(2): 203-213, 1996.

Fu M & Tupling AR. Heat shock protein hsp70 provides functional protection to the cardiac Ca^{2+} pump (sarco(endo)plasmic reticulum Ca^{2+}-ATPase 2a) against heat stress. *Appl. Physiol. Nutr. Metab.* 32 Supplement: S32, 2007.

Fujii J, Ueno A, Kitano K, Tanaka S, Kadoma M & Tada M. Complete complementary DNA-derived amino acid sequence of canine cardiac phospholamban. *J. Clin. Invest*. 79(1): 301-304, 1987.

Goloubinoff P & De Los Rios P. The mechanism of Hsp70 chaperones: (entropic) pulling the models together. *Trends Biochem. Sci.* 32(8): 372-380, 2007.

Gramolini AO, Kislinger T, Asahi M, Li W, Emili A & MacLennan DH. Sarcolipin retention in the endoplasmic reticulum depends on its C-terminal RSYQY sequence and its interaction with sarco(endo)plasmic Ca(2+)-ATPases. *Proc. Natl. Acad. Sci.* 101: 16807-16812, 2004.

Gramolini AO, Trivieri MG, Oudit GY, Kislinger T, Li W, Patel MM, Emili A, Kranias EG, Backx PH & MacLennan DH. Cardiac-specific overexpression of sarcolipin in phospholamban null mice impairs myocyte function that is restored by phosphorylation. *Proc. Natl. Acad. Sci.* 103: 2446-2451, 2006.

Green HJ, Düsterhöft S, Dux L & Pette D. Metabolite patterns related to exhaustion, recovery and transformation of chronically stimulated rabbit fast-twitch muscle. *Pflugers Arch.* 420(3-4): 359-366, 1992.

Grover AK, Samson SE & Fomin VP. Peroxide inactivates calcium pumps in pig coronary artery. *Am. J. Physiol*. 263(2 Pt 2): H537-H543, 1992.

Grover AK, Samson SE & Misquitta CM. Sarco(endo)plasmic reticulum Ca^{2+} pump isoform SERCA3 is more resistant than SERCA2b to peroxide. *Am. J. Physiol. Cell Physiol.* 273: C420-C425, 1997.

Gutiérrez-Martin Y, Martín-Romero FJ, Iñesta-Vaquera FA, Gutiérrez-Merino C & Henao F. Modulation of sarcoplasmic reticulum Ca^{2+}-ATPase by chronic and acute exposure to peroxynitrite. *Eur. J. Biochem.* 271: 2647-2657, 2004.

Harada Y, Sato C & Kitajima K. Complex formation of 70-kDa heat shock protein with acidic glycolipids and phospholipids. *Biochem. Biophys. Res. Commun*. 353(3): 655-660, 2007.

Hendrickson WA & Liu Q. Exchange we can believe in. *Structure*. 16(8): 1153-1155, 2008.

Hill CA, Thompson MW, Ruell PA, Thom JM & White MJ. Sarcoplasmic reticulum function and muscle contractile character following fatiguing exercise in humans. *J. Physiol.* 531: 871-878, 2001.

Holloway GP, Green HJ & Tupling AR. Differential effects of repetitive activity on sarcoplasmic reticulum responses in rat muscles of different oxidative potential. *Am. J. Physiol. Reg. Int. Comp. Physiol.* 290: R393-R404, 2006.

Holt E, Sjaastad I, Lunde PK, Christensen G & Sejersted OM. Thyroid hormone control of contraction and the Ca^{2+}-ATPase/phospholamban complex in adult rat ventricular myocytes. *J. Mol. Cell Cardiol.* 31(3): 645-656, 1999.

Hu P, Zhang KM, Spratt JA, Wechsler AS & Briggs FN. Transcription rates of SERCA and phospholamban genes change in response to chronic stimulation of skeletal muscle. *Biochim. Biophys. Acta* 1395(1): 121-125, 1998.

Hughes E, Clayton JC, Kitmitto A, Esmann M & Midrio A. Solid-state NMR and functional measurements indicate that the conserved tyrosine residues of sarcolipin are involved directly in the inhibition of SERCA1. *J. Biol. Chem.* 282: 26603-26613, 2007.

Inashima S, Matsunaga S, Yasuda T & Wada M. Effect of endurance training and acute exercise on sarcoplasmic reticulum function in rat fast- and slow-twitch skeletal muscles. *Eur. J. Appl. Physiol.* 89: 142-149, 2003.

Ishii T, Sunami O, Saitoh N, Nishio H, Takeuchi T & Hata F. Inhibition of skeletal muscle sarcoplasmic reticulum Ca2+-ATPase by nitric oxide. *FEBS Lett*. 440(1-2): 218-222, 1998.

Javed MU, Michelangeli F & Lund PA. GroEL protects the sarcoplasmic reticulum Ca(++)-dependent ATPase from inactivation in vitro. *Biochem. Mol. Biol. Int.* 47: 631-638, 1999.

Kaplan P, Babusikova E, Lehotsky J & Dobrota D. Free radical-induced protein modification and inhibition of Ca^{2+}-ATPase of cardiac sarcoplasmic reticulum. *Mol. Cell. Biochem.* 248: 41-47, 2003.

Khassaf M, Child RB, McArdle A, Brodie DA, Esanu C & Jackson MJ. Time course of responses of human skeletal muscle to oxidative stress induced by nondamaging exercise. *J. Appl. Physiol.* 90: 1031-1035, 2001.

Khor HK, Fisher MT & Schöneich C. Potential role of methionine sulfoxide in the inactivation of the chaperone GroEL by hypochlorous acid (HOCl) and peroxynitrite ($ONOO^-$). *J. Biol. Chem*. 279(19): 19486-19493, 2004.

Kimura Y, Asahi M, Kurzydlowski K, Tada M & MacLennan DH. Phospholamban domain Ib mutations influence functional interactions with the Ca2+-ATPase isoform of cardiac sarcoplasmic reticulum. *J. Biol. Chem*. 273(23): 14238-14241, 1998.

Kiss E, Jakab G, Kranias EG & Edes I. Thyroid hormone-induced alterations in phospholamban protein expression: Regulatory effects on sarcoplasmic reticulum Ca^{2+} transport and myocardial relaxation. *Circ. Res.* 75: 245-251, 1994.

Kissner R, Nauser T, Bugnon P, Lye PG & Koppenol WH. Formation and properties of peroxynitrite as studies by laser flash photolysis, high-pressure stopped-flow technique, and pulse radiolysis. *Chem. Res. Toxicol.* 10: 1285-1292, 1997.

Klebl BM, Ayoub AT & Pette D. Protein oxidation, tyrosine nitration, and inactivation of sarcoplasmic reticulum Ca2+-ATPase in low-frequency stimulated rabbit muscle. *FEBS Lett.* 422 (3): 381-384, 1998.

Knyushko TV, Sharov VS, Williams TD, Schöneich C & Bigelow DJ. 3-Nitrotyrosine modification of SERCA2a in the aging heart: A distinct signature of the cellular redox environment. *Biochemistry* 44: 13071-13081, 2005.

Kobzik L, Reid MB, Bredt DS & Stamler JS. Nitric oxide in skeletal muscle. *Nature* 372: 546-548, 1994.

Kumar M & Mitra D. Heat shock protein 40 is necessary for human immunodeficiency virus-1 Nef-mediated enhancement of viral gene expression and replication. *J. Biol. Chem*. 280(48): 40041-40050, 2005.

Laemmli UK. Cleavage of structural proteins during the assembly of the head of bacteriophage T4. *Nature*. 227(5259): 680-685, 1970.

Lees SJ, Franks PD, Spangenburg EE & Williams JH. Glycogen and glycogen phosphorylase associated with sarcoplasmic reticulum: effects of fatiguing activity. *J. Appl. Physiol.* 91: 1638-1644, 2003.

Leeuw T & Pette D. Coordinate changes of myosin light and heavy chain isoforms during forced fiber type transitions in rabbit muscle. *Dev. Genet.* 19 (2):163-168, 1996.

Leppik JA, Aughey RJ, Medved I, Fairweather I, Carey MF & McKenna MJ. Prolonged exercise to fatigue in humans impairs skeletal muscle Na^+-K^+-ATPase activity, sarcoplasmic reticulum Ca^{2+} release, and Ca^{2+} uptake. *J. Appl. Physiol.* 97: 1414-1423, 2004.

Li SY, Yang X, Ceylan-Isik AF, Du M, Sreejayan N & Ren J. Cardiac contractile dysfunction in Lep/Lep obesity is accompanied by NADPH oxidase activation, oxidative modification of sarco(endo)plasmic reticulum Ca2+-ATPase and myosin heavy chain isozyme switch. *Diabetologia*. 49(6): 1434-1446, 2006.

Liu Q & Hendrickson WA. Insights into Hsp70 chaperone activity from a crystal structure of the yeast Hsp110 Sse1. *Cell*. 131(1): 106-120, 2007.

Liu Y, Gampert L, Nething K & Steinacker JM. Response and function of skeletal muscle heat shock protein 70. *Front. Biosci*. 11: 2802-2827, 2006.

Lytton J & MacLennan DH. Molecular cloning of cDNAs from human kidney coding for two alternatively spliced products of the cardiac Ca^{2+}-ATPase gene. *J. Biol. Chem.* 263: 15024-15031, 1988.

MacLennan DH, Abu-Abed M & Kang C. Structure-function relationships in Ca^{2+} cycling proteins. *J. Mol.Cell. Cardiol.* 34: 897-918, 2002.

MacLennan DH, Brandl CJ, Korczak B, & Green NM. Amino-acid sequence of a Ca^{2+} + Mg^{2+}-dependent ATPase from rabbit muscle sarcoplasmic reticulum, deduced from its complementary DNA sequence. *Nature* 316: 696-700, 1985.

MacLennan DH, Yip CC, Iles GH & Seeman P. Isolation of sarcoplasmic reticulum proteins. *Cold Spring Harbor Symp. Quant. Biol.* 37: 469-478, 1972.

Mall S, Broadbridge R, Harrison SL, Gore MG, Lee AG & East JM. The presence of sarcolipin results in increased heat production by Ca^{2+}-ATPase. *J. Biol. Chem.* 281: 36597-36602, 2006.

Mandel F, Kranias EG, de Gende AC, Sumida M & Schwartz A. The effect of pH on the transient-state kinetics of Ca^{2+}-Mg^{2+}-ATPase of cardiac sarcoplasmic reticulum. A comparison with skeletal sarcoplasmic reticulum. *Circ. Res.* 50: 310-317, 1982.

Matsunaga S, Harmon S, Gohlsch B, Ohlendieck K & Pette D. Inactivation of sarcoplasmic reticulum Ca^{2+}-ATPase in low-frequency stimulated rat muscle. *J. Muscle Res. Cell Motil.* 22: 685-691, 2001.

Matsunaga S, Inashima S, Yamada T, Watanabe H, Hazama T & Wada M. Oxidation of sarcoplasmic reticulum Ca^{2+}-ATPase induced by high-intensity exercise. *Pflugers Arch.* 446: 394-399, 2003.

Mayer MP & Bukau B. Hsp70 chaperones: cellular functions and molecular mechanism. *Cell. Mol. Life. Sci*. 62(6): 670-684, 2005.

Milne KJ & Noble EG. Exercise-induced elevation of HSP70 is intensity dependent. *J. Appl. Physiol.* 93: 561-568, 2002.

Moreau VH, Castilho RF, Ferreira ST & Carvalho-Alves PC. Oxidative damage to sarcoplasmic reticulum Ca^{2+}-ATPase at submicromolar iron concentrations: Evidence for metal-catalyzed oxidation. *Free Radic. Biol. Med.* 25: 554-560, 1998.

Morita T, Hussain D, Asahi M, Tsuda T, Kurzydlowski K, Toyoshima C & Maclennan DH. Interaction sites among phospholamban, sarcolipin, and the sarco(endo)plasmic reticulum Ca(2+)-ATPase. *Biochem. Biophys. Res. Commun.* 369(1): 188-194, 2008.

Morth JP, Pedersen BP, Toustrup-Jensen MS, Sørensen TL, Petersen J, Andersen JP, Vilsen B & Nissen P. Crystal structure of the sodium-potassium pump. *Nature*. 450(7172): 1043-1049, 2007.

Morton JP, MacLaren DPM, Cable NT, Bongers T, Griffiths RD, Campbell IT, Evans L, Kayani A, McArdle A & Drust B. Time course and differential responses of the major heat shock protein families in human skeletal muscle following acute nondamaging treadmill exercise. *J. Appl. Physiol.* 101: 176-182, 2006.

Muller A, van Hardeveld C, Simonides WS & van Rijn J. Ca2+ homeostasis and fast-type sarcoplasmic reticulum Ca(2+)-ATPase expression in L6 muscle cells. Role of thyroid hormone. *Biochem. J*. 283 (Pt 3): 713-718, 1992.

Nielsen JS, Madsen K, Jørgensen LV & Sahlin K. Effects of lengthening contraction on calcium kinetics and skeletal muscle contractility in humans. *Acta Physiol. Scand.* 184: 203-214, 2005.

O'Brien PJ, Li GO, Locke M, Klabunde RE & Ianuzzo CD. Compensatory up-regulation of cardiac SR Ca2+-pump by heat-shock counteracts SR Ca2+-channel activation by ischemia/reperfusion. *Mol. Cell. Biochem*. 173(1-2): 135-143, 1997.

Odermatt A, Taschner PE, Scherer SW, Beatty B, Khanna VK, Cornblath DR, Chaudhry V, Yee WC, Schrank B, Karpati G, Breuning MH, Knoers N & MacLennan DH. Characterization of the gene encoding human sarcolipin (SLN), a proteolipid associated with SERCA1: absence of structural mutations in five patients with Brody disease. *Genomics* 45: 541-553, 1997.

Odermatt A, Becker S, Khanna VK, Kurzydlowski K, Leisner E, Pette D & MacLennan DH. Sarcolipin regulates the activity of SERCA1, the fast-twitch skeletal muscle sarcoplasmic reticulum Ca2+-ATPase. *J. Biol. Chem*. 273(20): 12360-12369, 1998.

Pan Y, Zvaritch E, Tupling AR, Rice WJ, de Leon S, Rudnicki M, McKerlie C, Banwell BL, & MacLennan DH. Targeted disruption of the ATP2A1 gene encoding the sarco(endo)plasmic reticulum Ca^{2+} ATPase isoform 1 (SERCA1) impairs diaphragm function and is lethal in neonatal mice. *J. Biol. Chem.* 278: 13367-13375, 2003.

Pette D & Düsterhöft S. Altered gene expression in fast-twitch muscle induced by chronic low-frequency stimulation. *Am. J. Physiol. Reg. Int. Comp. Physiol.* 262: R333-R338, 1992.

Protasi F. Structural interaction between RYRs and DHPRs in calcium release units of cardiac and skeletal muscle cells. *Front. Biosci.* 7: d650-d658, 2002.

Röckl KS, Witczak CA & Goodyear LJ. Signaling mechanisms in skeletal muscle: acute responses and chronic adaptations to exercise. *IUBMB Life*. 60(3): 145-153, 2008.

Ruell PA, Hoffman KM, Chow CM & Thompson MW. Effect of temperature and duration of hyperthermia on HSP72 induction in rat tissues. *Mol. Cell. Biochem.* 267: 187-194, 2004.

Sahlin K, Nielsen JS, Mogensen M & Tonkonogi M. Repeated static contractions increase mitochondrial vulnerability toward oxidative stress in human skeletal muscle. *J. Appl. Physiol.* 101: 833-839, 2006.

Saibil HR. Chaperone machines in action. *Curr. Opin. Struct. Biol.* 18(1): 35-42, 2008.

Salo DC, Donovan CM & Davies KJ. HSP70 and other possible heat shock or oxidative stress proteins are induced in skeletal muscle, heart, and liver during exercise. *Free Radic. Biol. Med.* 11: 239-246, 1991.

Scherer NM & Deamer DW. Oxidative stress impairs the function of the sarcoplasmic reticulum by oxidation of sulfhydryl groups in the Ca^{2+}-ATPase. *Arch. Biochem. Biophys.* 246: 589-601, 1986.

Seidler NM, Jona I, Vegh M & Martonosi A. Cyclopiazonic acid is a specific inhibitor of the Ca^{2+}-ATPase of sarcoplasmic reticulum. *J. Biol. Chem.* 264(30): 17816-17823, 1989.

Senisterra GA, Huntley SA, Escaravage M, Sekhar KR, Freeman ML, Borrelli M & Lepock JR. Destabilization of the Ca^{2+}-ATPase of sarcoplasmic reticulum by thiol-specific, heat shock inducers results in thermal denaturation at 37^{o}C. *Biochemistry* 36: 11002-11011, 1997.

Sharov VS, Dremina ES, Galeva NA, Williams TD & Schöneich C. Quantitative mapping of oxidation-sensitive cysteine residues in SERCA *in vivo* and *in vitro* by HPLC-electrospray-tandem MS: selective protein oxidation during biological aging. *Biochem. J.* 394: 605-615, 2006.

Sharov VS, Galeva NA, Knyushko TV, Bigelow DJ, Williams TD & Schöneich C. Two-dimensional separation of the membrane protein sarcoplasmic reticulum Ca-ATPase for high-performance liquid chromatography-tandem mass spectrometry analysis of posttranslational protein modifications. *Anal. Biochem.* 308: 328-335, 2002.

Shenoy R, Klein I & Ojamaa K. Differential regulation of the SR calcium transporters by thyroid hormone in rate atria and ventricles. *Am. J. Physiol. Heart Circ. Physiol.* 281(4): H1690-H1696, 2001.

Simonides WS, Thelen MH, van der Linden CG, Muller A & van Hardeveld C. Mechanism of thyroid-hormone regulated expression of the SERCA genes in skeletal muscle: implications for thermogenesis. *Biosci. Rep*. 21(2): 139-154, 2001.

Simonides WS & van Hardeveld C. An assay for sarcoplasmic reticulum Ca2(+)-ATPase activity in muscle homogenates. *Anal. Biochem*. 191(2): 321-331, 1990.

Sriram M, Osipiuk J, Freeman B, Morimoto R & Joachimiak A. Human Hsp70 molecular chaperone binds two calcium ions within the ATPase domain. *Structure*. 5(3): 403-414, 1997.

Sugita Y, Miyashita N, Yoda T, Ikeguchi M & Toyoshima C. Structural changes in the cytoplasmic domain of phospholamban by phosphorylation at Ser16: a molecular dynamics study. *Biochemistry*. 45(39): 11752-11761, 2006.

Tada M & Toyofuku T. SR Ca(2+)-ATPase/phospholamban in cardiomyocyte function. *J. Card. Fail*. 2(4 Suppl): S77-S85, 1996.

Thelen MH, Muller A, Zuidwijk MJ, van der Linden GC, Simonides WS & van Hardeveld C. Differential regulation of the expression of fast-type sarcoplasmic-reticulum Ca(2+)-ATPase by thyroid hormone and insulin-like growth factor-I in the L6 muscle cell line. *Biochem J*. 303 (Pt 2): 467-474, 1994.

Thompson HS, Maynard EB, Morales ER & Scordilis SP. Exercise-induced HSP27, HSP70 and MAPK responses in human skeletal muscle. *Acta Physiol. Scand.* 178: 61-72, 2003.

Thompson HS, Scordilis SP, Clarkson & Lohrer WA. A single bout of eccentric exercise increases HSP27 and HSC/HSP70 in human skeletal muscle. *Acta Physiol. Scand.* 171: 187-193, 2001.

Toyoshima C. Ion pumping by calcium ATPase of sarcoplasmic reticulum. *Adv. Exp. Med. Biol.* 592: 295-303, 2007.

Toyoshima C. Structural aspects of ion pumping by Ca(2+)-ATPase of sarcoplasmic reticulum. *Arch. Biochem. Biophys.* 476(1): 3-11, 2008.

Toyoshima C, Asahi M, Sugita Y, Khanna R, Tsuda T & MacLennan DH. Modeling of the inhibitory interaction of phospholamban with the Ca2+ ATPase. *Proc. Natl. Acad. Sci.* 100(2): 467-472, 2003.

Toyoshima C, Nakasako M, Nomura H, & Ogawa H. Crystal structure of the calcium pump of sarcoplasmic reticulum at 2.6 Å resolution. *Nature* 405: 647-655, 2000.

Traaseth NJ, Ha KN, Verardi R, Shi L, Buffy JJ, Masterson LR & Veglia G. Structural and dynamic basis of phospholamban and sarcolipin inhibition of Ca(2+)-ATPase. *Biochemistry*. 47(1): 3-13, 2008.

Trost SU, Omens JH, Karlon WJ, Meyer M, Mestril R, Covell JW & Dillmann WH. Protection against myocardial dysfunction after a brief ischemic period in transgenic mice expressing inducible heat shock protein 70. *J. Clin. Invest.* 101: 855-862, 1998.

Tupling AR, Bombardier E, Stewart RD, Vigna C & Aqui AE. Muscle fiber type-specific response of Hsp70 expression in human quadriceps following acute isometric exercise. *J. Appl. Physiol*. 103(6): 2105-2111, 2007.

Tupling AR, Gramolini AO, Duhamel TA, Kondo H, Asahi M, Tsuchiya SC, Borrelli MJ, Lepock JR, Otsu K, Hori M, MacLennan DH & Green HJ. HSP70 binds to the fast-twitch skeletal muscle sarco(endo)plasmic reticulum Ca^{2+}-ATPase (SERCA1a) and prevents thermal inactivation. *J. Biol. Chem.* 279: 52382-52389, 2004.

Tupling R, Green H, Grant S, Burnett M & Ranney D. Postcontractile force depression in humans is associated with an impairment in SR Ca^{2+} pump function. *Am. J. Physiol. Reg. Int. Comp. Physiol.* 278: R87-R94, 2000.

Tupling R, Green H & Tupling S. Partial ischemia reduces the efficiency of sarcoplasmic reticulum Ca2+ transport in rat EDL. *Mol. Cell. Biochem*. 224(1-2): 91-102, 2001.

Tupling AR, Vigna C, Ford RJ, Tsuchiya SC, Graham DA, Denniss SG & Rush JW. Effects of buthionine sulfoximine (BSO) treatment on diaphragm contractility and SR Ca^{2+} pump function in rats. *J. Appl. Physiol.* 103(6): 1921-1928, 2007.

Uppu RM. Synthesis of peroxynitrite using isoamyl nitrite and hydrogen peroxide in a homogeneous solvent system. *Anal. Biochem*. 354(2): 165-168, 2006.

Uppu RM & Pryor WA. Synthesis of peroxynitrite in a two-phase system using isoamyl nitrite and hydrogen peroxide. *Anal. Biochem*. 236(2): 242-249, 1996.

Van Der Linden CG, Simonides WS, Muller A, Van Der Laarse WJ, Vermeulen JL, Zuidwijk MJ, Moorman AF, & Van Hardeveld C. Fiber-specific regulation of Ca^{2+}-ATPase isoform expression by thyroid hormone in rat skeletal muscle. *Am. J. Physiol. Cell Physiol*. 271: C1908-C1919, 1996.

Vangheluwe P, Schuermans M, Zádor E, Waelkens E, Raeymaekers L & Wuytack F. Sarcolipin and phospholamban mRNA and protein expression in cardiac and skeletal muscle of different species. *Biochem. J.* 389: 151-159, 2005.

Vega VL, Rodríguez-Silva M, Frey T, Gehrmann M, Diaz JC, Steinem C, Multhoff G, Arispe N & De Maio A. Hsp70 translocates into the plasma membrane after stress and is released into the extracellular environment in a membrane-associated form that activates macrophages. *J. Immunol*. 180(6): 4299-4307, 2008.

Viner Ri, Ferrington DA, Williams TD, Bigelow DJ & Schöneich C. Protein modification during biological aging: selective tyrosine nitration of the SERCA2a isoform of the sarcoplasmic reticulum Ca2+-ATPase in skeletal muscle. *Biochem. J.* 340: 657-669, 1999b

Viner RI, Krainev AG, Williams TD, Schöneich C & Bigelow DJ. Identification of oxidation-sensitive peptides within the cytoplasmic domain of the sarcoplasmic reticulum Ca^{2+}-ATPase. *Biochemistry* 36: 7706-7716, 1997.

Viner RI, Williams TD & Schöneich C. Nitric oxide-dependent modification of the sarcoplasmic reticulum Ca-ATPase: Localization of cysteine target sites. *Free Radic. Biol. Med.* 29: 489-496, 2000.

Viner RI, Williams TD & Schöneich C. Peroxynitrite modification of protein thiols: Oxidation, nitrosylation, and S-Glutathiolation of functionally important cysteine residue(s) in the sarcoplasmic reticulum Ca-ATPase. *Biochemistry* 38: 12408-12415, 1999a.

Wawrzynow A, Theibert JL, Murphy C, Jona I, Martonosi A & Collins JH. Sarcolipin, the "proteolipid" of skeletal muscle sarcoplasmic reticulum, is a unique, amphipathic, 31-residue peptide. *Arch. Biochem. Biophys*. 298(2): 620-623, 1992.

Welch WJ. Mammalian stress response: Cell physiology, structure/function of stress proteins, and implications for medicine and disease. *Physiol. Rev.* 72: 1063-1081, 1992.

Wu B, Hunt C & Morimoto R. Structure and expression of the human gene encoding major heat shock protein HSP70. *Mol. Cell. Biol*. 5(2): 330-341, 1985.

Wu KD & Lytton J. Molecular cloning and quantification of sarcoplasmic reticulum Ca(2+)-ATPase isoforms in rat muscles. *Am. J. Physiol. Cell Physiol.* 264: C333-C341, 1993.

Xu KY, Zweier JL & Becker LC. Hydroxyl radical inhibits sarcoplasmic reticulum Ca^{2+}-ATPase function by direct attack on the ATP binding site. *Circ. Res.* 80: 76-81, 1997.

Xu S, Ying J, Jiang B, Guo W, Adachi T, Sharov V, Lazar H, Menzoian J, Knyushko TV, Bigelow D, Schöneich C & Cohen RA. Detection of sequence-specific tyrosine nitration of manganese SOD and SERCA in cardiovascular disease and aging. *Am. J. Physiol. Heart Circ. Physiol.* 290: H2220-H2227, 2006.

Yamada T, Inashima S, Matsunaga S, Nara I, Kajihara H & Wada M. Different time course of changes in sarcoplasmic reticulum and myosin isoforms in rat soleus muscle at early stage of hyperthyroidism. *Acta Physiol. Scand.* 180: 79-87, 2004.

Yamashita N, Hoshida S, Nishida M, Igarashi J, Taniguchi N, Tada M, Kuzuya T & Hori M. Heat shock-induced manganese superoxide dismutase enhances the tolerance of cardiac myocytes to hypoxia-reoxygenation injury. *J. Mol. Cell. Cardiol*. 29(7): 1805-1813, 1997.

Ying J, Sharov V, Xu S, Jiang B, Gerrity R, Schöneich C & Cohen RA. Cysteine-674 oxidation and degradation of sarcoplasmic reticulum Ca(2+) ATPase in diabetic pig aorta. *Free Radic. Biol. Med*. Published online, Jun 13, 2008.

Zweier JL. Measurement of superoxide-derived free radicals in the reperfused heart. Evidence for a free radical mechanism of reperfusion injury. *J. Biol. Chem*. 263(3): 1353-1357, 1988.

Appendix A:
Homogenizing buffer recipe

Homogenizing buffer

Reagent	Molecular Weight (g/mol)	Mass (g)	Concentration (mM)
Sucrose	342.3	85.575	250
HEPES	238.3	1.1915	5
PMSF	174.19	0.034838	0.2
NaN_3	65.01	2.0	0.2%*

*NOTE: 1g solute per 100mL of H_2O = 1% solution

-Add PMSF to ~800 mL H_2O in a beaker with magnetic stir bar. Cover with parafilm and stir on a hot plate set at a temperature of 35-40^oC.

-Once PMSF has dissolved add the remaining reagents and pH to 7.5 with KOH, bring to **1 L** and re-check the pH.

Appendix B:
Synthesis of $ONOO^-$

Reagent	Concentration (M)	Volume (μL)	Temperature (^oC)	Incubation Time (min)
H_2O_2	10.3	1942	4	10
NaOH	5	4000	4	10
EDTA	0.04	500	4	10
H_2O	----	500	4	10
Isopentyl Nitrite	96%	5860	25	180

-The first 4 reagents were combined in a beaker with a magnetic stir bar and mixed vigorously in an ice-water mixture for 10 minutes.

-Subsequently, the beaker was removed from the ice-water mixture, isopentyl nitrite was added and the reaction proceeded for 180 min at room temperature.

-The concentration of $ONOO^-$ was calculated using the extinction coefficient 1670 $M^{-1} \cdot cm^{-1}$ and the following equation:

$$\frac{(\text{Abs. } ONOO^- \text{ 302nm} - \text{Abs. Blank})}{1670} * 1000 * 2 * \frac{1000}{2} = [ONOO^-]\ \text{mM}$$

Appendix C:
Microsomal Ca^{2+}-ATPase activity buffer

Assay buffer

Reagent	Molecular Weight (g/mol)	Mass (g)	Concentration (mM)
KCl	74.56	1.6024	100
HEPES	238.3	1.0243	20
NaN_3	65.01	0.1397	10
EGTA	380.4	0.08175	1
$MgCl_2$	95.21	0.2046	10
PEP	465.3*	1.0	10

*NOTE: The PEP used was a tricyclohexylammonium salt.

-Combine all reagents in a beaker with magnetic stir bar and ~190 mL H_2O.

-Heat to >37^{o}C and pH to 7.0 with KOH at 37^{o}C.

-Bring to **215 mL** and re-check pH. Store in 50 mL tubes at -20^{o}C

Appendix D:
Buffers used for co-immunoprecipitation

2X co-IP buffer

Reagent	Molecular Weight (g/mol)	Mass (g)	Concentration (mM)
NaCl	58.44	0.4383	300
HEPES	238.3	0.2383	40
EDTA	372.24	0.01861	2
$MgCl_2$	95.21	0.0238	10
1% Tween	----	250 µL	1%
PMSF*	174.19	400 µL	4

*NOTE: A 250 mM stock solution of PMSF was made in EtOH just prior to use. 400 µL were added to the final volume to give a PMSF concentration of 4 mM.

-In ~20 mL H_2O combine all reagents and pH to 7.5. Bring to **25 mL** and re-check pH. Store without PMSF (see note) at -20^oC until use.

1X co-IP buffer

-This buffer contains the same reagents listed above, but at half the concentration. Therefore, mass the reagents accordingly. NOTE: **100 mL** were made for these experiments.

Wash buffer

Reagent	Molecular Weight (g/mol)	Mass (g)	Concentration (mM)
NaCl	58.44	0.4383	150
Tris	121.14	0.1514	25

-Combine reagents in ~47 mL H_2O, pH to 7.2, bring to **50 mL** and re-check pH. Store at -20^oC.

Elution buffer

Reagent	Molecular Weight (g/mol)	Mass (g)	Concentration (mM)
Glycine	75.07	0.075	100

-Add glycine to ~5 mL H_2O, pH to 2.8, bring to **10 mL** and re-check pH. Store at -20^oC.

Neutralizing buffer

Reagent	Molecular Weight (g/mol)	Mass (g)	Concentration (M)
Tris	121.14	1.2114	1

-Add Tris to ~3-5 mL H_2O, pH to 9.0, bring to **10 mL** and re-check pH. Store at -20^oC.

Appendix E:
Buffers used for immunoprecipitation

2X IP buffer

Reagent	Molecular Weight (g/mol)	Mass (g)	Concentration (mM)
Tris	121.14	0.06057	20
Sucrose	342.3	5.1345	600
CHAPS	614.88	0.25	1%
1 tablet of Complete© Roche protease inhibitor was added to the buffer			

-Add reagents to ~10-15mL H_2O, pH to 7.4, bring to **25 mL** and re-check pH. Store at -20^{o}C.

1X IP buffer

-This buffer contains the same reagents listed above, but at half the concentration. Therefore, mass the reagents accordingly. NOTE: **100 mL** were made for these experiments.

Appendix F:
Buffers for FITC binding

1X FITC non-denaturing lysis buffer

Reagent	Molecular Weight (g/mol)	Mass (g)	Concentration (mM)
NaCl	58.44	0.17532	300
Tris	121.14	0.06057	50
EDTA	372.24	0.01861	5
NaN_3	65	0.002	0.02%
Triton-X	----	100 µL	1%
PMSF*	174.19	40 µL	1

*NOTE: A 250 mM stock solution of PMSF was made in EtOH just prior to use. 40 µL were added to the final volume to give a PMSF concentration of 1 mM.

-Combine all reagents in ~8 mL H_2O, pH to 7.4, bring to **10 mL** and re-check pH. Store at -20°C.

FITC binding buffer

Reagent	Molecular Weight (g/mol)	Mass (g)	Concentration (mM)
Tris-HCl	157.6	0.788	50
$CaCl_2$	110.98	0.00111	0.1
$MgCl_2$	95.21	0.0476	5
Sucrose	342.3	8.5575	250
FITC	389.38	*	0.02
1 tablet of Complete© Roche protease inhibitor was added to the buffer per 50 mL			

*NOTE: A FITC stock solution (6.42 mM) was made in ethanol and stored at -70°C until use.

-Combine all reagents in ~70 mL H_2O, pH to 8.8, bring to **100 mL** and re-check pH. Store at -20°C

-To achieve a FITC concentration of 0.02 mM, 3.12 µL of FITC were added to 997 µL of binding buffer just prior to use.

Appendix G:
Buffers used for derivation of reactive carbonyls

Derivatization buffer

Reagent	Molecular Weight (g/mol)	Mass (g)	Concentration (mM)
2,4-DNPH	198.14	0.019814	10

-Dissolve 2,4-DNPH in **10 mL of 2 M HCl** and store at room temperature, protected from light.

Neutralization buffer

Reagent	Molecular Weight (g/mol)	Mass (g)	Concentration (M)
Tris	121.14	2.4228	2
Glycerol	-----	3 mL	30%

-Combine glycerol, ~2 mL H_2O and Tris. Heat to ~40^{o}C to help dissolve Tris. Bring to final volume with water, **do not** pH and store at -20^{o}C.